MEMBRANE DEVELOPMENT FOR METAL IONS AND ANIONS SEPARATION

LU JUNWEN

(B.Eng., M. Eng.)

A THESIS SUBMITTED
FOR THE MASTER'S DEGREE OF ENGINEERING

DEPARTMENT OF CHEMICAL & BIOMOLECULAR ENGINEERING
NATIONAL UNIVERSITY OF SINGAPORE

2007

ACKNOWLEDGEMENTS

I would like to express my sincere gratitude, first and foremost, to my supervisor, Professor Tai-Shung Chung, for his patient, generous and constructive guidance, continuous inspirations and encouragements in the course of this study.

I am fortunate to be a research student in Professor Tai-Shung Chung's group. Thanks to the remarkable people and outstanding academic environment in Professor Tai-Shung Chung's group, my experience as a research student at NUS has been pleasurable and fruitful.

I am also grateful to invaluable suggestions and help from Assistant Professor Jiang Jianwen and Dr Yang Qian, Dr Wang Kaiyu, Dr Li Yi, Dr Jiang Lanying, Dr Teo May May, Dr Qiao Xiangyi, Dr Xiao Youchang in the course of my study.

Finally, I would like to express my heartiest gratitude to my family in China for their sacrifice, understanding and support over these years.

TABLE OF CONTENTS

SUMMARY

The purpose of this research work is to develop a novel method to select carrier for supported liquid membrane systems to remove cadmium and to investigate the separation performance of a novel amphoteric PBI nanofiltration hollow fiber membrane for wastewater treatment.

Theoretical prediction of the extraction capabilities for three kinds of carriers (Aliquat 336, Kelex 100 and LIX 54) for cadmium in supported liquid membrane (SLM) systems using the quantum chemical computation method has been carried out in this work. The single point energy calculation results show that the energy changes in the complex formation process are in the order of Aliquat 336/Cd(II) > Kelex 100/Cd(II) > LIX 54/Cd(II), with energy changes of -657.79, -329.19 and 96.32 kcal/mol, respectively. This prediction has been well verified by SLM flux as a function of carrier concentration in the membrane phase with the maximum fluxes of Aliquat 336, Kelex 100, LIX 54 being 1.12×10^{-9}, 1.5×10^{-10} and 7.9×10^{-11} mol/(cm^2·s), respectively. This research work indicate that quantum chemical computation can be proposed for carrier selection in supported liquid membrane (SLM) systems for heavy metal ions removal. Generally, the more negative energy change for the carrier/Cd(II) system indicates the more favorable process for the formation of the complex and consequently the better the extraction capability of the carrier. FTIR results also agree with the computational prediction quite well. Investigation on the influence of stirring rate and strippant on the cadmium flux reveals that a stirring rate of 400 rpm and the use of 1 mM EDTA as the strippant

constitute the optimal experimental conditions. It was also found that cadmium flux is a function of feed concentration at the low concentration stage and the cadmium flux is enhanced by appropriate addition of certain anion into the feed. This indicated that in the supported liquid membrane systems, heavy metal transmembrane flux can be enhanced effectively (with a flux increase by 91% in our case) by adding only small amount of anion(s) with less negative free energy of hydration.

The feasibility of the removal of both anions (phosphate, arsenate and borate ions) and cations (copper ions) by employing a novel amphoteric polybenzimidazole (PBI) nanofiltration (NF) hollow fiber membrane has also been investigated. The membrane structure, charge characteristics and ion rejection performance of the fabricated PBI NF hollow fiber membrane have been systematically studied. The surface charge characterization of PBI membranes indicate that the PBI NF membranes have an isoelectric point near pH 7.0 and therefore have different charge signs based on the media pH due to the amphoteric structure of imidazole group within PBI molecules. This unique charge characteristic makes the PBI membrane a good candidate for the removal of both cations and anions, where the PBI membrane exhibits different charge signs at adjustable pH. Investigations on the rejection capability of typical anions, e.g. phosphate, arsenate and borate ions and typical heavy metal cations, e.g. copper ions, reveal that the PBI NF membrane exhibits better rejection performance for various ion removal. Their rejections are strongly dependent on the chemical nature of electrolytes, solution pH and the feed concentrations. The experimental results are analyzed by using the Speigler-Kedem model with the transport parameters of the reflection coefficient (σ) and the solute

permeability (P). The PBI NF membrane may have a potential industrial utility in the removal of various environmentally-unfriendly species.

LIST OF TABLES

LIST OF FIGURES

NOMENCLATURE

$A_k/\Delta x$	ratio of membrane porosity over thickness (m^{-1})
C_b	concentration in the bulk solution (mol m^{-3})
C_f	feed concentration (mol m^{-3})
C_m	concentration at the membrane surface (mol m^{-3})
C_p	concentration in permeate (mol m^{-3})
$\bar{c}$	Logarithmic average concentration (mol m^{-3})
D_s	the diffusivity of solute molecule in a dilute solution (m^2 s^{-1})
D_i	diffusivity of ion i in free solution (m^2 s^{-1})
J_s	solute or ion flux (mol m^{-2} s^{-1})
J_v	permeate flux (based on membrane area) (m^3 m^{-2} s^{-1})
L_P	pure water permeability (m^3 m^{-1} s^{-1} bar^{-1})
P	solute permeability (m s^{-1})
ΔP	applied trans-membrane pressure difference (bar)
P'	local solute permeability (m s^{-1})
r_p	effective pore radius (m)
r_s	Stoke radius of ion (m)
R_{obs}	observed rejection (%)
R_T	real rejection (%)

Greek letters

α	the transport number of cation in free solution defined as $\alpha = D_1/(D_1+D_2)$
σ	reflection coefficient (–)

φX effective membrane charge (mol m^{-3})

ξ the ratio of effective volume charge density (ϕ X) of membrane to the electrolyte concentration (C_m) at the membrane surface (–)

$\Delta\pi$ Osmotic pressure difference (bar)

Subscript

a anion

c cation

1. CHAPTER ONE

INTRODUCTION

1.1 General Background Information

In the 21st century, water resources have been the limiting factor for human development due to the growing population and increasing environmental pollution of the existing water resources [1].

The pollution of groundwater, rivers and lakes with contaminants caused large amount of wastewater. Wastewater may encompass a wide range of potential contaminants, such as toxic species, oxygen demanding wastes, pathogenic agents, organic & inorganic chemicals and minerals and sediments [2]. A continuously increasing world population as well as higher quality standards and expenses for drinking water make water treatment for water reuse an effective way to reduce water consumption. Therefore, wastewater treatment is very crucial for a lower water consumption.

1.2 Conventional Wastewater Treatment Processes

1.2.1 Adsorption

Adsorption is the concentration of a substance at the interface or surface [3]. The adsorption at the interface or surface is largely due to binding forces between ions, atom and molecules of the adsorbate on the sorbent surface [4]. An ideal adsorbent should have

a very strong affinity for the target contaminants, and simultaneously have the ability to release the adsorbate from the adsorbent under a different condition so that the adsorbent can be regenerated.

Since cost is an important consideration for selection adsorbent materials, natural materials, such as biopolymeric sorbent vermiculite and clays which are readily available in large quantities, cheap and environmentally-friendly have recently been paid increasing attention [5-8]. The commercial adsorbents used for the removal of contaminants from wastewater include a variety of gels, activated carbon, silica, activated alumina, zeolites, ion exchange resin and other resinous materials [9-13]. For example, activated alumina and ion exchange resin have been demonstrated to be effective in removing arsenic from water. Several different sorbents such as natural clays and biopolymeric sorbent vermiculite have been investigated in terms of decontamination of the discharged effluents and concentration of heavy metal ions [5-8]. The adsorption methods are confronted with some problems, such as poor selectivity and slow regeneration.

1.2.2 Electrocoagulation

In electrocoagulation process, the coagulant is produced by electrolytic oxidation of a certain anode material [14] and colloid matters are coagulated and separated with the direct current. During the electrocoagulation process, hydrogen gas evolution at cathode is accompanied with metal anode's dissolution. The main advantages of

electrocoagulation are simple and can be easily operated. Wastewater treated by electrocoagulation produced clear, colorless, and odorless water. Furthermore, flocs generated by electrocoagulation can be treated easily and they are de-waterable. Main disadvantage of electrocoagulation is that anode electrodes need to be regularly replaced due to the dissolution of electrodes with oxidation. Another disadvantage is high conductivity of the water suspension is required and high usage of electricity is needed during the process [14]. The electrocoagulation process can be used in municipal or industrial wastewater treatment plants (WWTP) as well as in water treatment.

1.2.3 Ion Exchange

During the ion exchange process, exchange between counter ion on bead surface and ion in the solution with the different electrostatic force is reversibly occurred. In the process, cation, such as copper, nickel, cadmium, is exchanged with H^+. Also, anion, as chlorides, sulfates and chromates is exchanged with OH^-. This technology has been mainly used for water softening, pharmaceutical purification, production of ultra-pure water for semiconductor processes, purification in the food industry, etc. Ion exchange processes have also been demonstrated to remove heavy metal ions including copper and cadmium from the wastewater effectively [15, 16]. For ion exchange processes, it is difficult to develop novel ion exchange resins with highly selective functional groups for greater selectivity for the removal of contaminants alone.

1.2.4 Solvent Extraction

Solvent extraction is a well known wastewater treatment for its ability to selectively separate and concentrate metals [17]. However, the solvent extraction process suffers from drawbacks, such as a large amount of solvent consumption, solvent degradation and inadequate decontamination efficiency [18].

1.2.5 Precipitation

Precipitation is a conventional process for wastewater treatment. This process offers a non-contaminating approach for wastewater treatment since the purposely added chemicals into the wastewater are generally precipitated out together with the contaminant.

In comparison with aforementioned conventional wastewater treatment processes, membrane processes provide a number of advantages including higher standards, the potential for mobile treatment units and decreased environmental impact of effluents. Membrane processes are competitively efficient in removing particulate and dissolved contaminants, including microorganisms and toxic species.

1.3 Pressure Driven Membrane Processes for Wastewater Treatment

Pressure-driven membrane processes as a wastewater treatment process have drawn an increasing attention. Various processes of pressure driven membrane processes, including microfiltration, ultrafiltration, nanofiltration and reverse osmosis can be used to purify a dilute solution. During these membrane processes, the solvent and various solute ions or/and molecules permeate through the membrane, whereas other particles and molecules or ions are retained to some extent dependent on the membrane structures. The pore sizes of the membranes become smaller from microfiltration through ultrafiltration and nanofiltration to reverse osmosis. Decision of which pressure-driven membrane process should be used is dependent on the chemical composition of waste to be removed.

1.3.1 Microfiltration (MF)

Microfiltration (pore sizes between 0.1 and 10μm) is typically used in drinking water treatment for the removal of particulate material，inorganic particles and the natural organic materials in the range 0.1–2.0μm [19, 20]. Microfiltration may also be act as a pre-treatment step before a more retentive membrane process such as nanofiltration (NF) or reverse osmosis (RO).

In a conventional microfiltration process "dead-end filtration" during which the feed flow to the filter is perpendicular to its surface, is often used. This kind of microfiltration suffers from one disadvantage: the particles are retained on the surface of the membrane during the microfiltration, resulting in resistance to the permeate flow. In order to address this drawback, "crossflow microfiltration" (CFMF) where in the direction of feed flow is

made parallel to the surface of the filter has been modified from "dead-end filtration". Therefore, the resistance created by the retained particles on the membrane surface is reduced, thus resulting in a higher rate of throughput. Treatment of industrial wastewaters containing toxic heavy metal ions has been carried out with crossflow microfiltration. The performance has also been quantified and the comparison with traditional technologies for wastewater treatment has also been carried out [21]. Some of the important advantages of using CFMF in water treatment are: 1. Stable and high product water quality, 2. Bacterial decontamination without chemical addition. 3. Economical for small water supply systems. 4. Ultrapure water for industrial purposes. However, CFMF suffers disadvantage such as permeate flux decline with time, resulting from many phenomena such as concentration polarization, fouling, deposition, membrane compression, gel layer formation, internal clogging, etc.

1.3.2 Ultrafiltration (UF)

Ultrafiltration is a low-pressure membrane process used for fractionation of selected components by size, whose nature lies between microfilteration and nanofiltration. The pore size of ultrafiltration membranes range from 0.05 μm to 1nm. Ultrafiltration (UF) is used to remove a variety of small impurities in the production of natural protein products, blood components, recombinant proteins and industrial enzymes [22]. It also provides an excellent removal performance of all protozoan cysts of concern and most bacteria. Other applications can be found in paper industry, textile industry, metallurgy, leather industry and chemical industry [23, 24]. Among pressure-driven membrane technologies,

ultrafiltration process possesses special aspects in drinking water processes because of its capability of providing quality water at a relatively modest cost of capital and operation [25]. Moreover, some successful examples confirm the significance of ultrafiltration process, in which the UF process acts as the pretreatment for RO process [26, 27].

1.3.3 Nanofiltration (NF)

The nature of nanofiltration process lies between those of ultrafiltration and reverse osmosis membranes and characterized by pore diameters of the order of nanometers. Compared to reverse osmosis membranes, the network of nanofiltration membranes is more open, enabling higher fluxes with lower pressures. Therefore, nanofiltration systems operate at a lower pressure (about half the pressure required for a reverse osmosis system) but retaining the same flux, resulting in lower energy costs and investment savings on lower pressure pump and piping. In addition, this kind of membrane structure implies that the retention of multivalent ions (Cu^{2+}, Cd^{2+} and SO_4^{2-}) is higher than monovalent ions (Na^+ and Cl^-) which are rather harmless. Compared to ultrafiltration membranes, nanofiltration membranes have a tighter structure and therefore have the ability to reject small organic molecules with molecular weights. It permits the retention of small molecules in the molecular mass range of 200 to 2000 Da.

Nanofiltration has two interesting features: one is that the MWCOs (molecular weight of the solute that is 90% rejected by the membrane) range from 200 to 1000 due to the pore diameters ranging from 0.5 nm to 2 nm; another one is that most of NF membranes are

either positively-charged or negatively-charged [28]. Therefore, the NF separation mechanisms involve both steric-hindrance and electrostatic (Donnan) effects. For the separation of uncharged solutes, size effect is the governing factor to determine the solute permeation. However, the NF processes to separate the charged ions are mainly determined by the electrostatic interaction between the solute species and the charged NF membranes. Hence, for the transport of charged solutes, the membrane charge characteristics play a significant role. Due to this reason, for wastewater treatment aimed at the removal of charged heavy metals, nanofiltration is an increasingly attractive process. The performance of the nanofiltration separation process is determined by many factors including surface charge characteristics and the type of the nanofiltration membrane, feed pH, operating pressure, feed flowrate, temperature, membrane module configuration, feed concentration and percentage product recovery [29–35].

1.3.4 Reverse Osmosis

Reverse osmosis is a membrane separation process that use generated pressure to force clean water through a membrane and consequently removes dissolved salts and contaminants, including chemicals, viruses and bacteria [36-38]. It is commonly used for wastewater treatment in the metal plating industry. Spatz [39] developed a novel method for recovering gold and rinsing water in an electroplating process with a reverse osmosis membrane. Hewitt and Dando [40] developed a reverse osmosis water recycling system for the treatment of contaminated water from rinsing baths. Sugita [41] invented a process for the recovery of precious metals such as gold with reverse osmosis process.

This process utilized a reverse osmosis membrane system to recover the metal salt from a wastewater stream. The metal ion was further concentrated with ion exchange columns.

Many other authors have also reported the application of reverse osmosis to reduce TDS, hardness, nitrates, cyanides, fluorides, arsenic, heavy metals, salinity, colour and organic compounds, e.g., biological oxygen demand (BOD), chemical oxygen demand (COD), total organic carbon (TOC), total organic halides (TOX), trihalomethanes (THM), and pesticides, besides the elimination of bacteria, viruses, turbidity and TSS from surface water, groundwater, and seawater [42-76].

A high flowrate is often used to reduce fouling. The high flowrate combined with higher operating pressures results in a higher energy requirement than other types of membranes.

Membrane fouling, a complex phenomenon involving the deposition of organic, inorganic and biological material in the form of colloidal suspensions or particulates on the membrane surface, is a major problem of reverse osmosis process and it can have several negative effects: a decrease in water production because of a gradual decline in flux, an increase in applied pressure required for a constant rate of water production, a gradual membrane degradation which results in a shorter membrane life, decreased salt rejection [77].

1.4 Membrane Process using concentration difference as driving force for Wastewater Treatment---Supported Liquid Membrane (SLM)

In SLM, organic extractant, carrier, is imbedded in small pores of a polymer support and is kept there by capillary forces. The carrier usually binds selectively with targeted species in the feed phase and transports the species into the strip phase. If the organic liquid is immiscible with the aqueous feed and strip streams, SLM can be used to separate the two aqueous phases. It also contain a diluent which is generally an inert organic solvent to adjust viscosity and sometimes also a modifier to avoid so called third phase formation. The mechanism of supported liquid membrane is given in Figure 1.1. The following separated steps can be distinguished: (1) Dissolving of solute in the liquid membrane; (2) Complexation of the solute with the carrier at the feed phase/membrane interface; (3) The formed carrier-solute complex diffuses across the membrane; (4) Decomplexation of carrier-solute complex at the membrane/ stripping phase interface; (5) Release of the solute from the membrane phase in the stripping phase; (6) The carrier diffuses back to the feed phase/membrane interface.

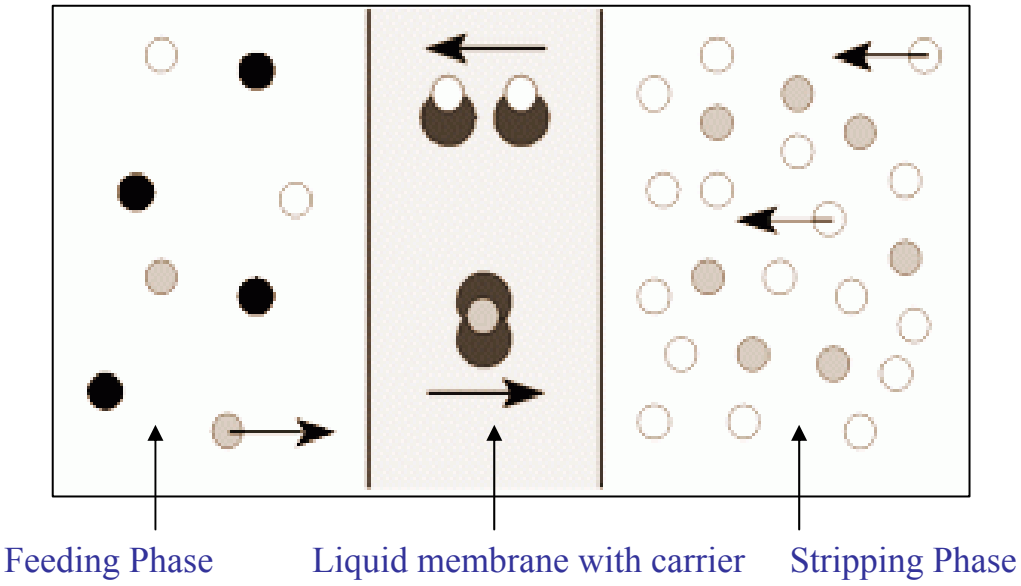

Figure 1.1 The mechanism of supported liquid membrane with mobile carrier

From the mechanism of the SLM, we can see that SLM process is somewhat similar to the solvent extraction process but with extraction and back-extraction performed in just one technological step. And supported liquid membrane extraction targets and removes the solute from bulk solutions based on chemical potential rather than by size difference, unlike the aforementioned pressure-driven membrane processes.

Supported liquid membranes have received considerable attention due to characteristics such as ease of operation, low energy consumption, operation cost, high selectivity and rapid extraction capacity factors. Because of these factors, supported liquid membranes have been proposed as an alternative to liquid–liquid extraction, chromatography and ion exchange for separation and purification [78-80]. From a practical point of view, separation membranes find applications in the industrial [81, 82], biomedical, and analytical fields as well as in wastewater treatment [83-86].

1.5 Thermally Driven Membrane Process for Wastewater Treatment—Membrane Distillation

Membrane distillation is a thermally driven process involving transport of water vapour through the pores of hydrophobic membranes due to a transmembrane vapor pressure difference driving force provided by temperature and/or concentration differences across a membrane. The liquid feed to be treated by MD must be in direct contact with one side of the membrane and does not penetrate inside the dry pores of the membranes. In order to prevent liquid solutions from entering its pores, the hydrophobic membranes are used

in this process [87, 88]. And consequently, only volatile components of the feed may be transported through the membrane in the membrane distillation process.

In the process of membrane distillation, the membrane only acts as a barrier to hold the liquid/vapor interfaces at the entrance of the membrane pores and it does not necessarily possess the ability of selection. The requirements for membrane distillation process are that the membrane must not be wetted and only vapor are present within membrane pores. To avoid pore wettability, the membrane material must be hydrophobic with high pure water contact angle. Normally, hydrophobic membranes are made from polyvinylidene fluoride (PVDF), polytetrafluoroethylene (PTFE), polyethylene (PE), polypropylene (PP).

The main advantage of membrane distillation over the traditional distillation process is that membrane distillation can work with a large surface area per volume as can be found in hollow fiber and capillary modules [89].

1.6 Research Objectives and Outline of the Thesis

Removal of toxic ions from dilute wastewater effluents through supported liquid membrane process has gained particular interest due to the advantages that this membrane technology offers many advantages, such as operational simplicity, low organic phase inventory, low energy consumption, high selectivity, etc.

Cadmium is mainly obtained as a by-product in the metallurgical processing of other metals such as copper, zinc and lead. Despite its toxicity, cadmium and its alloys are used in various industries such as chemicals, electroplating, electronics and other industries. Usually most often cadmium-bearing species enter the water system through industrial discharge and the poisoning by the metal or its compounds occurs through inhalation and ingestion. Therefore, it is important to removal cadmium and its alloys from liquid effluents to maintain a safer environment.

The use of liquid membrane systems for cadmium transport had been reported in the literature [92-95], but apparently little comparison of computational study of membrane extraction for cadmium (II) in supported liquid membrane (SLM) systems with experimental study has been carry out. In this research work, experimental and computational studies on transport of cadmium through a supported liquid membrane will be investigated in order to further understand fundamental kinetics and mechanistic study of cadmium transfer through SLM system.

Nanofiltration as a relatively new pressure-driven membrane process is also a significant membrane process for toxic ions removal because NF separation mechanisms involve not only steric-hindrance effect but also electrostatic (Donnan) effects, promising NF an effective method for charged ions removal. For the separation of uncharged solutes, size effect is the governing factor to determine the solute permeation. NF processes to separate the charged ions are mainly determined by the electrostatic interaction between the solute species and the charged NF membranes. There are a lot of investigations have

been done to evaluate the separation performance of cations, e.g. copper, and anions, e.g. borate ion, phosphate, arsenate or arsenite using respective NF membranes [94-97]. Generally, positively-charged NF membranes are only effective for cations removal, whereas negatively-charged NF membranes are only effective for anions removal. There is few amphoteric nanofiltration membranes reported which could exhibit different charges at different pH ranges, subsequently show efficient separation performance on both cations and anions based on the solution pH. Another objective of this work is to investigate the charge characteristics of a novel amphoteric polybenzimidazole (PBI) NF membrane and explore the potential of PBI NF membranes using as candidate membrane for the removal of both cations and anions which are environmentally concerned.

In order to achieve the objectives, the scopes of this work have been drawn as follows:

1. Fundamentally understand kinetics and mechanistic study of heavy metal transfer through SLM system
2. Investigate the nanofiltration membrane charge properties
3. Explore the potential of PBI NF membranes using as candidate membrane for the removal of both cations and anions

General conclusions drawn from this thesis are summarized in Chapter Five. Inclusive in this ending chapter are some recommendations and suggestions for future research.

References

[1] Y. Yoshinobu, R. Ehara, I. Sigeru and G. Totaro, Ion-exchange membrane electrodialytic salt production using brine discharged from a reverse osmosis seawater desalination plant. *J. Membr. Sci.* **222** (2003) 71.

[2] Metcalf and Eddy, Wastewater Engineering: Treatment, Disposal, Reuse. New York: McGraw-Hill, 1979.

[3] Barrow, G.M.: Physical Chemistry, sixth edn., McGraw-Hill, North America (1996) 344.

[4] Levine, I.N.: Physical Chemistry, fourth edn. McGraw-Hill, North America, 1995.

[5] K.H. Chu, M.A. Hashim, Adsorption of copper (II) and EDTA-chelated copper (II) onto granular activated carbons, *J. Chem. Technol. Biot.* **75** (2000) 1054-1060.

[6] N.Y. Dho, S.R. Lee, Effect of temperature on single and competitive adsorptions of Cu(II) and Zn(II) onto natural clays, *Environ. Monit. Assess.* **83** (2003) 177-203.

[7] N. Unlu, M. Ersoz, Adsorption characteristics of heavy metal ions onto a low cost biopolymeric sorbent from aqueous solutions, *J. Hazard. Mater.* **136** (2006) 272-280.

[8] G. Abate, J.C. Masini, Influence of pH, ionic strength and humic acid on adsorption of Cd(II) and Pb(II) onto vermiculite, *Colloid Surface A* **262** (2005) 33-39.

[9] Westrich, H.R., Cygan, R.T., Brady, P.V., Nagy, K.L., Anderson, H.L.: Sorption Behaviour of Cs and Cd onto Oxide and Clay Surfaces, Govt. Reports, Announcements and Index (GRA&I), Issue-18 (1995).

[10] Puls, R.W., Bohn, H.L.: Sorption of Cd(II), Ni(II) and Zn(II) by kaolinite and montmorillonite suspensions, *Soil Sci. Soc. Amer. J.* **52** (1988) 1289–1292.

[11] Orumwense, F.F.O.: Removal of lead from water by adsorption on a kaolinitic clay, *J. Cem. Technol. Biotechnol.* **65** (1996) 363–369.

[12] Qadeer, R., Hanif, J., Saleem,M., Afzal,M.: Adsorption of gadolinium on activated-charcoal from electrolytic aqueous solution. *Nucl. Chem. Articles* **159**(1992) 155–165.

[13] Saleem, M., Afzal, M., Qadeer, R., Hanif, J.: Selective adsorption of uranium on activated-charcoal rom electrolytic aqueous solutions. *Sep. Sci. Tech.* **27**(1992) 239–253.

[14] M.Y.A. Mollah, R. Schennach, J.R. Parga and D.L. Cocke, Electrocoagulation (EC)—science and applications, *J. Hazard. Mater.* **B84** (2001) 29–41.

[15] M. A. Keane, The removal of copper and nickel from aqueous solution using Y zeolite ion exchangers, *Colloid Surface A* **138** (1998) 11-20.

[16] W.M. Wang, V. Fthenakis, Kinetics study on separation of cadmium from tellurium in acidic solution media using ion-exchange resins, *J. Hazard. Mater.* **125** (2005) 80-88.

[17] Deorkar, N.V.; Tavlarides, L.L. Zinc, cadmium, and lead separation from aqueous streams using solid-phase extractants. *Ind. Eng. Chem. Res.* **36**(1997) 399–406.

[18] J.S. Liu, H. Chen, X.Y. Chen, Z.L. Guo, Y.C. Hu, C.P. Liu and Y.Z. Sun, Extraction and separation of In(III), Ga(III) and Zn(II) from sulfate solution using extraction resin, *Hydrometallurgy* **82** (2006) 137-143.

[19] A.I. Schafer, U. Schwicker, M.M. Fischer, A. Fane, T.D. Waite, Microfiltration of colloids and natural organic matter, *J. Membr. Sci.* **171** (2000) 151.

[20] V. Starov, D. Lloyd, A. Filippov, S. Glaser, Sieve mechanism of microfiltration separation, *Sep. Purif. Tech.* **23** (2002) 51.

[21] G.P.Brooma, R.C.Squiresb, M.P.J.Simpsonb and I. Martin, The treatment of heavy metal effluents by crossflow microfiltration. *J. Membr. Sci.* **87** (1994) 219-230.

[22] Madsen R.F. Design of sanitary and sterile UF and diafiltration plants, *Sep. Purif. Tech.* **22** (2001) 79– 87.

[23] Eykamp, W.: Microfiltration and Ultrafilteration, in Nobel, R.D., and Stern,S.A.,(eds), Membrane Separationa Technology. Principles and Applications, Elsevier, Amsterdam, 1995.

[24] Cheryan, Ultrafiltration Handbook, Technomic Publishing Co, Lancaster, USA, 1986.

[25] H. Choi, H.S. Kim, I.T. Yeom and D.D. Dionysiou, Pilot plant study of an ultrafiltration membrane system for drinking water treatment operated in the feed-and-bleed mode, *Desalination* **172** (2005) 281–291.

[26] J.J. Qin, M.H. Oo, H. Lee, and R. Kolkman, Dead-end ultrafiltration for pretreatment of RO in reclamation of municipal wastewater effluent. *J. Membr. Sci.* **243** (2004) 107–113.

[27] W. Bonnelye, M.A. Sanz, J.P. Durand, L. Plasse, F. Gueguen, and P. Mazounie, Reverse osmosis on open intake seawater: Pre-treatment strategy. *Desalination* **167** (2004) 191–200.

[28] K. K. Sirkar, Membrane separation technologies: Current developments, *Chem. Eng. Commun.* **157** (1997) 145-184.

[29] P. Eriksson, Nanofiltration extends the range of membrane filtration, *Environ. Prog.* **7** (1988) 58.

[30] R. Rautenbach, A. Groschl, Separation potential of nanofiltration membranes, *Desalination* **7** (1990) 73.

[31] L.P. Raman, M. Cheryan, N. Rajagopalan, Consider nanofiltration for membrane separations, *Chem. Eng. Prog.* **90** (1994) 68.

[32] M. Meireles, A. Bessieres, I. Rogissart, P. Aimar, V. Sanchez, An appropriate molecular size parameter for porous membranes calibration, *J. Membr. Sci.* **103** (1995) 105.

[33] X.L. Wang, T. Tsuru, M. Togoh, S.I. Nakao, S. Kimura, Evaluation of pore structure and electrical properties of nanofiltration membranes, *J. Chem. Eng. Jpn.* **28** (1995) 186.

[34] W.R. Bowen, H. Mukhtar, Characterisation and prediction of separation performance of nanofiltration membranes, *J. Membr. Sci.* **112** (1996) 263.

[35] B. Van der Bruggen, J. Schaep, D. Wilms, C. Vandecasteele, Influence of molecular size, polarity and charge on the retention of organic molecules by nanofiltration, *J. Membr. Sci.* **156** (1999) 29.

[36] Y. Watanabe, Y. Kanemoto, K. Takeda and H. Ohmo, Removal of soluble and particulate organic material in municipal water-water by a chemical flocculation and biofilm processes. *Water Sci. Tech.* **27** (1993) 201.

[37] P.L. McCarty, D. Argo, M. Reinhard, J. Graydon, N. Goodman and M. Aieta, Proc., Water Reuse Symposium, Washington, DC, USA, 2 (1981) 2325.

[38] G. Inoue, H. Ogasaware, C. Yanagi and Y. Muray ama, Advanced treatment of secondary sewage effluent by membrane process. *Desalination* **39** (1981) 423.

[39] D.D. Spatz, Metal reclamation process and apparatus, US Patent 3637467 (1972).

[40] D.E. Hewitt, T.J. Dando, Water recycle treatment system for use in metal processing, US Patent, 3973987 (1975).

[41] N. Sugita, Process and apparatus for recovery of precious metal compound, US Patent 4880511 (1989).

[42] C . Ventresque and G . Bablon, The integrated nanofiltration system of the Mery sur-Oise surface water treatment plant, *Desalination* **113** (1997) 263-266.

[43] R. Boussahel, S. Bouland, K.M. Moussaoui and A. Montiel, Removal of pesticide residues in water using the nanofiltration process, *Desalination* **132** (2000) 205-209.

[44] S. Bertrand, I. Lemaitre and E. Wittmann, Performance of a nanofiltration plant on hard and highly sulphated water during two years of operation, *Desalination* **113** (1997) 277-281.

[45] J. Bohdziewicz, M. Bodzek and E. Wasik, The application of reverse osmosis and nanofiltration to the removal of nitrates from groundwater, *Desalination* **121** (1999) 139-147.

[46] P. Berg, G. Hagmeyer and R. Gimbel, Removal of pesticides and other micropollutants by nanofiltration, *Desalination* **113** (1997) 205-208.

[47] S. Choi, Z. Yun, S. Hong and K. Ahn, The effect of co-existing ions and surface characteristics of nanomembranes on the removal of nitrate and fluoride, *Desalination* **133** (2001) 53-64.

[48] J.A. Redondo, Brackish-, sea- and wastewater desalination, *Desalination* **138**(2001) 29-40.

[49] B. Ericsson and B. Hallmans, Membrane applications in raw water treatment with and without reverse osmosis desalination, *Desalination* **98** (1994) 3-16.

[50] B. Ericsson, M. Hallberg and J. Wachenfeldt, Nanofiltration of highly colored raw water for drinking water production, *Desalination* **108** (1996)129-141.

[51] I .C. Escobar, S. Hong and A .A. Randall, Removal of assimilable organic carbon and biodegradable dissolved organic carbon by reverse osmosis and nanofiltration membranes, *J . Membr. Sci.* **175** (2000) 1-17.

[52] Y. Garba, S. Taha, N. Gondrexon, J. Cabon and G. Dorange, Mechanisms involved in cadmium salts transport through a nanofiltration membrane: characterization and distribution, *J . Membr. Sci.* **168** (2000) 135-141.

[53] A. Hafiane, D. Lemordant and M. Dhahbi, Removal of hexavalent chromium by nanofiltration, *Desalination* **130** (2000) 305-312.

[54] J.A.M.H. Hofman, E.F. Beerendonk, H.C. Folmer and J.C. Kruithof, Removal of pesticides and other micropollutants with cellulose-acetate, polyamide and ultra-low pressure reverse osmosis membranes, *Desalination* **113** (1997) 209-214.

[55] S. Kimura, Analysis of reverse osmosis membrane behaviors in a long-term verification test, *Desalination* **100** (1995) 77-84.

[56] Y . Kiso, Y . Nishimura, T . Kitao and K . Nishimura, Rejection properties of non-phenylic pesticides with nanofiltration membranes, *J. Membr. Sci.* **171** (2000) 229-237.

[57] Y. Kiso, Y . Sugiura, T . Kitao and K . Nishimura, Effects of hydrophobicity and molecular size on rejection of aromatic pesticides with nanofiltration membranes, *J. Membr. Sci* . **192** (2001) 1-10.

[58] Z.V. P. Murthy and S .K. Gupta, Sodium cyanide separation and parameter estimation for reverse osmosis thin film composite polyamide membrane, *J. Membr. Sci* .**154** (1999) 89-103.

[59] R. Rautenbach, T. Linn and D.M.K. Al-Gobaisi, Present and future pretreatment concepts-strategies for reliable and low-maintenance reverse osmosis seawater desalination, *Desalination* **110** (1997) 97-106.

[60] R. Rautenbach and A. Groschl, Separation potential of nanofiltration membranes, *Desalination* **77** (1990) 73-84.

[61] A.G. Pervov, Y.V. Reztsov, S.B. Milovanov, V.S. Koptev and A .G . Melnikov, Production of quality drinking water with membranes, *Desalination* **108** (1996) 167-170.

[62] W.J. Conlon, Pilot field test data for prototype ultra low pressure reverse osmosis elements, *Desalination* **56** (1985) 203-226.

[63] J.A. Redondo, Development and experience with new FILMTEC reverse osmosis membrane elements for water treatment, *Desalination* **108** (1996) 59-66.

[64] E. Wittmann, P. Cote, C. Medici, J. Leech and A.G. Turner, Treatment of a hard borehole water containing low levels of pesticide by nanofiltration, *Desalination* **119** (1998) 347-352 .

[65] B. Van der Bruggen, J. Schaep, W. Maes, D. Wilms and C. Vandecasteele, Nanofiltration as a treatment method for the removal of pesticides from ground waters, *Desalination* **117** (1998) 139-147.

[66] H. Winters, Twenty years experience in seawater reverse osmosis and how chemicals in pretreatment affect fouling of membranes, *Desalination* **110** (1997)93-96.

[67] J.S. Taylor, D .M. Thompson and J .K. Carswell, Applying membrane processes to groundwater sources for trihalomethane precursor control, *J. AWWA* **79** (1987) 72-82.

[68] B. Van der Bruggen, J . Schaep, D . Wilms and C. Vandecasteele, Influence of molecular size, polarity and charge on the retention of organic molecules by nanofiltration, *J . Membr. Sci* . **156** (1999) 29-41.

[69] G.L. Amy, B .C. Alleman and C.B. Cluff, Removal of dissolved organic matter by nanofiltration, *J. Environ. Eng.* **116** (1990) 200-205.

[70] C. Ventresque, V. Gisclon, G. Bablon and G. Chagneau, An outstanding feat of modem technology: the Mery-sur-Oise nanofiltration treatment plant, *Desalination* **131** (2000) 1-16.

[71] N.G. Voros, Z .B. Maroulisand and D. Marinos- Kouris, Salt and water permeability in reverse osmosis membranes, Desalination **104** (1996) 141-154.

[72] C.K. Yeom, S.H. Lee and J.M. Lee, Effect of the ionic characteristics of charged membranes on the permeation of anionic solutes in reverse osmosis, *J. Membr. Sci.* **169** (2000) 237-247.

[73] B. Van der Bruggen, K. Everaert, D. Wilms and C. Vandecasteele, Application of nanofiltration for removal of pesticides, nitrate and hardness from ground water: rejection properties and economic evaluation, *J . Membr. Sci.* **193** (2001) 239-248.

[74] G.T. Szabo, G. More and Y. Ramadan, Filtration of organic solutes on reverse osmosis membrane. Effect of counter-ions, *J. Membr. Sci.* **118** (1996) 295-302.

[75] A. Yaroshchuk and E. Staude, Charged membranes for low pressure reverse osmosis properties and applications, *Desalination* **86** (1992) 115-134.

[76] B.M. Watson and C .D. Homburg, Low-energy membrane nanofiltration for removal of color, organics and hardness from drinking water supplies, *Desalination* **72** (1989) 11-22 .

[77] K. Karakulski and W.A. Morawski, Purification of copper wire drawing emulsion by application of UF and RO, *Desalination* **131** (2000) 87–95.

[78] Green, (Eds.), Perry's Chemical Engineers' Handbook, McGraw-Hill Book Co, Singapore, 1984.

[79] R. Wodzki, G. Sionkowski, Recovery and concentration of metal ions. II Multimembrane hybrid system, *Sep. Sci. Technol.* **30** (1995), 2763.

[80] V. S. Kislik, A. M. Eyal Hybrid liquid membrane (HLM) system in separation technologies, *J. Membr. Sci.* **111***(*1996) 259.

[81] P. R. Danesi, E. P. Horwitz, G. F. Vandegrift, R. Chiarizia, Mass transfer rate through liquid membranes: Interfacial chemical reactions and diffusion as simultaneous permeability controlling factors, *Sep. Sci. Technol.* **16** (1981) 201.

[82] P. R. Danesi, L. Reichley-Vinger, P. G. Rickert, Lifetime of supported liquid membranes: The influence of interfacial properties, chemical composition and water transport on the long-term stabilities of the membranes, *J. Membr. Sci.* **31**(1987) 117.

[83] R. Prasad, A. Kiani, R. R. Bhave, K. K Sirkar, Further studies on solvent extraction with immobilized interfaces in a microporous hydrophobic membrane, *J. Membr. Sci.* **26** (1986) 79.

[84] R. Prasad, K. K. Sirkar, Solvent extraction with microporous hydrophilic and composite membranes, *AIChE J.* **33** (1987) 1057.

[85] R. Prasad, K. K. Sirkar, Microporous membrane solvent extraction, *Sep. Sci. Technol.* **22** (1987) 619.

[86] I. J. Youn, Y Lee, W. H. Lee, Analysis of permeation rate of cobalt ions across a supported liquid membrane containing HEH- (EHP), *J. Membr. Sci*. **100** (1995) 69.

[87] A.C.M. Franken, J.A.M. Nolten, M.H.V. Mulder, D. Bargeman, C.A. Smolders, Wetting criteria for the applicability of membrane distillation, *J. Membr. Sci.* **33** (1987) 285–298.

[88] K.W. Lawson, D.R. Lloyd, Membrane distillation, *J. Membr. Sci.* **124** (1997) 1–25.

[89] Marcel Mulder 2nd Edn, Basic principles of membrane technology. Kluwer Academic Publishers. The Netherlands.

[90] R.J. Marr, J. Draxler, in: W.S. Ho, K.K. Sirkar (Eds.), Membrane Handbook. Van Nostrand Reinhold, New York, 1992.

[91] M. Akhond, M. Shamsipur, Specific uphill transport of Cd^{2+} ion by a cooperative carrier composed of aza-18-crown-6 and palmitic acid. *J. Membr. Sci.* **117** (1996) 221.

[92] V.A. Daimininger, A.G. Geist, W. Nitsch, P.K. Plucinski, Efficiency of hollow fiber modules for nondispersive chemical extraction. *Ind. Eng. Chem. Res.* **35** (1996)184.

[93] A. Almela, M.P. Elizalde, K. Kamel, in: D.C. Shallcross, R. Paimin, L. Prvcic (Eds.), Value Adding Through Solvent Extraction (Proceedings of ISEC ’96), vol. 2, The University of Melbourne, Melbourne, 1996.

[94] H. Saitua, M. Campderros, S. Cerutti, A.P. Padilla, Effect of operating conditions in removal of arsenic from water by nanofiltration membrane, *Desalination* **172** (2005) 173-180.

[95] M.C. Shih, An overview of arsenic removal by pressure-driven membrane processes, *Desalination* **172** (2005) 85-97.

[96] S.M.C. Ritchie, D. Bhattacharyy, Membrane-based hybrid processes for high water recovery and selective inorganic pollutant separation, J. Hazard. Mater. **92** (2002) 21-32.

[97] R. Simons, Trace element removal from ash dam waters by nanofiltration and diffusion dialysis. *Desalination* **89** (1993) 325-341.

2. CHAPTER TWO

LITERATURE REVIEW

2.1 Metal Ions Removal by Supported Liquid Membrane

2.1.1 Introduction

Supported liquid membranes (SLM), which draws inspiration from facilitated transport in life science, e.g., oxygen transport through haemoglobin [1], has been used widely for the separation of ions [2-3]. In the SLM process, an organic phase containing a carrier separates two aqueous phases, one being the feed phase containing the species to be transported, say metal ions, and the other being the stripping phase. Liquid membrane is the organic phase which is immiscible with both aqueous phases. The carrier molecules chosen are those have finite solubility in the organic phase (the liquid membrane phase) and are insoluble to some extent in both aqueous phases and have strong affinity for the ions or molecules to be transported. The commonly accepted mechanism of the transport process in SLM systems is the following:

The species, such as metal ions, are partitioned into the liquid membrane phase in the feed phse/membrane interface where they complex with the carrier. This complex travels from feed phase/membrane interface to the membrane/stripping phase interface where it decomplexes and the metal ions diffuse into the stripping phase. The carrier molecules travels back to the membrane/feed phase interface where it again complexes with the metal ions, and so on.

2.1.2 Modeling of SLM Transport Mechanisms for Metal Ions Removal

The development of theoretical models accounting for the experimental results is essential to completely understand SLM transport mechanisms. Theoretical models provide explanation of the experimental results but also offer prediction of the behavior and performance of a system under different experimental conditions when experimental and system parameters are given (concentration of chemical in phases, forward and reverse rate constants, the membrane thickness, mass transfer coefficients of the species to be transported in the membrane, etc.). Such models have been proposed and applied in supported liquid membrane, both in flat sheet and hollow fiber configurations.

A number of models have been proposed for various conditions such as interfacial complexation and decomplexation, mass transfer resistances within the membrane and different morphology and structures for flat sheet supported liquid membranes and hollow fiber supported liquid membrane and active transport, passive transport and diffusion have been extensively reviewed [4, 5]. A nonequilibrium approach addressing the transport in boundary layers of the aqueous liquid film has also been disscussed [6-8].

The transport of the metals ion through the supported liquid membrane system is considered to be composed of many elementary steps, expressed as follows [9-17]:

(1) Diffusion of metal ions from the bulk feed phase to the aqueous stagnant layer on the feed phase side. (2) Complexation reactions between the carrier ligand and metal ions to be transported at the feed phase/membrane interface. (3) Transport of the formed

complex within the membrane from the feed phase/membrane interface to the stripping phase/membrane interface. (4) Release of the metal ion-carrier complex at the stripping interface. (5) The released metal ion diffuses from the stripping phase interface to the bulk phase across the aqueous diffusional layer. (6) Diffusion of the free carrier back to the feed phase/membrane interface. Considering the co- or countertransport of the chemical species serving as the driving forces for the transport process, additional steps can be included in the reaction mechanism: (7) The co- or counter species diffuse across the aqueous diffusional layers. (8) The co-or counter species react with the carrier ligand.

In the description of the transport model, the following assumptions have been made: the complexation at the feed phase/membrane and decomplexation at stripping phase/membrane interface are fast; the diffusion of ions in both aqueous film layers is also fast; and the diffusion of carrier and regenerated carrier between feed phase/membrane interface and the stripping phase/membrane interface can be neglected. It is also assumed that all the diffusion processes can be determined by Fick's diffusion equations. At the steady state, the metal flux density, N_M, across the supported liquid membrane for each step is expressed as follows [18, 19].

1. Diffusion of metal ions from the bulk of feed phase to the aqueous stagnant layer in the feed side [18, 19],

$$N_M=(D_M/\delta)_f\ ([M^{+2}]_f-[M^{+2}]_{i,1}\ )=k_f\ ([M^{+2}]_f-[M^{+2}]_{\ i,1}) \qquad (2.1)$$

Where D_M is the diffusion coefficient of metal ion in the feed phase, δ is the film layer thickness, and k_f is the mass transfer coefficient of aqueous boundary layer at the feed phase side.

2. Diffusion of metal ion-carrier complex from the membrane/feed phase interface to the stripping phase/membrane interface [18, 19],

$$N_M = (D_{R2M}, b^{\varepsilon}) ([R_2M]_{i,1} - [R_2M]_{i,2})/l\tau^2 = k_m([R_2M]_{i,1} - [R_2M]_{i,2}) \quad (2.2)$$

Where D_{R2M} is the diffusion coefficient of the metal complex in the organic phase, ε is the porosity of membrane, τ is the tortuosity of the memrbane and l is the thickness of the membrane.

3. Diffusion of metal ion from the stripping phase/membrane interface to the bulk stripping phase [18, 19],

$$N_M = (D_M/\delta)_s ([M^{+2}]_{i,2} - [M^{+2}]_s) = k_s([M^{+2}]_{i,2} - [M^{+2}]_s) \quad (2.3)$$

k_s is the mass transfer coefficient of aqueous boundary layer at the side of stripping phase. By rearrangement of Eqs. 2.1-2.3 the transport rate model of metal ion through supported liquid membrane can be obtained.

2.1.3 Application of SLM for Heavy Metal Removal

Table 2.1 summarizes the various extraction systems with Flat-Sheet SLM, including the removed ion, feed phase, stripping phase and carrier/dilute. From Table 2.1, one can see

that (1) SLM systems are effective way for heavy metal removal; (2) in order to obtain an effective SLM system, it is crucial to use proper stripping phase and carrier/dilute [20-49].

Table 2.1 Review of Extraction Systems with Flat-Sheet SLM

Ions	Feed	Strip	carrier/diluent
Ca(II)	Cl-	0.001-0.1 M HNO_3	HDEHP/*n*-dodecane
Co(II)	SO_4^{2-}	H_2SO_4	HEH(EHP)/kerosene
Co(II), Ni(II)	1 M $LiNO_3$, HNO_3	1 M $LiNO_3$, HNO_3	HEH(EHP)/kerosene
Co(II), Ni(II)	0.5 M Na_2SO_4, pH 3-5	0.9 N H_2SO_4	HDEHP/kerosene
Co(II), Ni(II), Cu(II)	NaAC+HAC, pH 5.0	H_2SO_4, pH 2.3	D2EHPA/kerosene
Cs(I)	1 M HNO3, 5.8 M $LiNO_3$ + 1 M HNO_3	H_2O	DB21C7, B21C7, tBuB21C7, nDecB21C7/*n*-hexylbenzene
Cu(II)	0.01 M $LiClO_4$, pH 6.0	$NaNO_3$, $Na_4P_2O_4$ in 0.01 M LiOH,	22DD + HDEP/ toluene + kerosene
Cu(II)	1.9 M NaAcO + 0.1 M AcOH, pH 6.0	2 M H_2SO_4	HDEHP/dodecane
Cu(II)	sulfate, pH= 2.63	0.5-2.0 M H_2SO_4	AcorgaP-50/*n*-octane, mesitylene
Cu(II)	1.47 M NH_3, pH = 11	1.5 M H_2SO_4	LIX 84/kerosene
Cu(II)	NaAC+HAC, pH 6-7	1 M H_2SO_4	tetradentate hydroxamate/$CHBr_3$
Cu(II), Cd(II), Cd(II)	NaAC+HAC	2 wt % HCl	LIX 84/kerosene
Cd(II)	0-0.8 M LiCl	water	bathocuproine/dibenzyl ether
Cd(II), Ni(II),	I^-, NO_3^-, Br^-, Cl^-	water	tetradentate oxoiminato
Cd(II), Cr(VI)	Cd^{2+} : 1 M NaCl	water	Cd^{2+} : Alamine

Cr(III)	sulfate, pH= 4.2-4.5	water	Cr^{3+} : DNNSA/*o*-xylene, kerosene, *n*-heptane, kerosene-*o*-xylene
Ga(III)	synthetic Bayer liquor	1.5 M HCl	Kelex100 + Versatic 10/kerosene
Ga(III)	various pH values (0.5-6.0)	pH 0.5	ODPHA/kerosene
Hg(II)	0.001-0.03 M $NaNO_2$, pH 1-10	0.001-0.009 M $Na_2S_2O_3$, pH 1-10	18C6, DC18C6, DB18C6, DA18C6, 15C5, DA15C5/CHCl3
Hg(II), Ag(I)	HNO_3, $HClO_4$	1 M H_2SO_4,	BTPD/kerosene, dodecane
Hg(II)	$HgCl_2$	DI water	LPB/NPOE
Mn(II)	0.009 M Na_2SO_4+ acetate, pH 2-4.5	9 M H_2SO_4	D2EHPA/kerosene
Mo(VI)	0.001-0.1 M HCl, pH 1-3	0.01-1 M NaOH	TOA/xylene
Mo(VI)	0.001-0.1 M HCl	0.01-1 M NaOH	TOA/xylene
Na(I), K(I), Rb(I)	nitrate solution	DI water	DC18C6 + 2-NPOE + T2BEP + CTA + MeCl
Ni(II)	0.1 M HAC+NaAC	0.1 M HNO_3	D2EHPA/*n*-dodecane
Au(III), Ir(IV), Pd(II), Pt(II), Ru	0.1-5 M HCl	0.1-4 M HNO_3	TOA/kerosene
Pd(II)	0.5 M HCl	0.1-4 M HNO_3, 0.1-3 M $HClO_4$	TOA/kerosene
Pd(II)	0.01-3 M HCl	2 M aqueous NH_3	DETE/toluene
Sr(II)	synthetic solution	DI water	DC18C6/various
Se(IV)	2.25×10^{-3} M HCl	0.24 M H_2O_2 in 10^{-3} HCl	Na(DDTC)/kerosene
Ti(IV)	1-3 M H_2SO_4	0.1-2.5 M NH_4F	D2EHPA/CCl_4
U(VI)	H_2SO_4, pH 2.0	HEDPA	CYANEX272/*n*-dodecane

V(IV)	0.5 M Na_2SO_4+H_2SO_4, pH 1.3-2.5	pH 0.58-0.94	D2EHPA/kerosene
Y(III), Fe(III)	0.01 M H_2SO_4	1 M H_2SO_4	EHPA/kerosene
Zn(II)	0.1 M LiCl	DI water	bathocuproine/dibenzyl ether
Zn(II)	HAC+NaAC, pH 4.7	0.1 M HCl	CYANEX 272 /dodecane

2.2 Wastewater Treatment by Nanofiltration

2.2.1 Mechanism of Nanofiltration Separations

NF separation mechanisms involve both steric-hindrance and electrostatic (Donnan) effects. For the separation of uncharged solutes, size effect is the governing factor to determine the solute permeation. However, the NF processes to separate the charged ions are mainly determined by the electrostatic interaction between the solute species and the charged NF membranes. Hence, for the transport of charged solutes, the membrane charge characteristics play a significant role. Due to this reason, for wastewater treatment aimed at the removal of charged heavy metals, nanofiltration is an increasingly attractive process. Since the membrane charge characteristics play a significant role during the transport of charged solutes, the investigation of the membrane charge properties is of great importance.

2.2.2 Applications of Nanofiltration for Water & Wastewater Treatment

The history of nanofiltration (NF) dates back to 30 years ago because reverse osmosis membranes use a considerable energy cost and produce very good, or often even too good quality water. Due to this reason, nanofiltration membranes with a reasonable water flux operating at relatively low pressures were developed. In the past decade, nanofiltration process has been extensively investigated for water and wastewater treatment and proved to be effective for removal of inorganic matters, inorganic matters, organic micropollutants and viruses and bacteria [50-92].

The feasibility of utilizing nanofiltration for like oil/water separation by NF has been investigated [93]. The investigation shows that nanofiltration can provide better separation than ultrafiltration without sacrificing flux.

Hardness removal is still one of the most important purposes of nanofiltration today. The comparison between nanofiltration and lime softening for groundwater treatment has been conducted [94]. It shows the product quality is the most important advantage of nanofiltration. Product quality of nanofiltration is superior to that of lime softening due to the additional removal of color and turbidity. Other advantages of nanofiltration are the the smaller land requirements, flexibility, the absence of sludge to dispose.

Actually, the removal of natural organic matter (NOM) is significant for most water treatment units and it can be done by nanofiltration effectively. Even though efficiency of

organics removal was lower than with reverse osmosis membranes, NF membranes still possess the capability of removing natural organic matter (NOM) and color [95-98].

The application of nanofiltration for pesticides removal has been investigated by many authors [99-104]. The removal efficiencies varied a lot dependent on the nanofiltration membranes and the kind of the pesticides to be removed. A more extensive investigation on organic micropollutants removal has been conducted by Hofman et al. [103]. In this study, comparison of the rejection of four different mixtures of micropollutants with ultralow pressure reverse osmosis membranes and with tight nanofiltration membranes has been invesigated.

Nanofiltration is also one of the important processes that can be used to meet regulations to decrease arsenic concentrations in drinking water [105]. The removal of Arsenic from surface water sources and from synthetic freshwater by RO and NF has been investigated by Waypa et al. [106]. Both As (III) and As (V) have been effectively rejected by RO and tight NF membranes (NF70, Dow/Filmtec) with various operational conditions.

References

[1] P.F. Scholander, Oxygen transport through hemoglobin solutions, *Science* **131** (1960) 585.

[2] J.J. Christensen, J.D. Lamb, S.R. Izatt, S.E. Starr, G.C. Weed, M.S. Astin, B.D. Slitt and R.M. Izatt, Effect of anion type on rate of facilitated transport of cations across liquid membranes via neutral macrocyclic carriers, *J. Am. Chem. Sot.* **100** (1978) 3219.

[3] R.M. Izatt, D.K. Roper, R.L. Bruening and J.D. Lamb, Macrocycle mediated cation transport using hollow fiber supported liquid membranes, *J. Membrane Sci.* **45** (1989) 73.

[4] R. D. Noble, J.D. Way, Liquid membrane technology: An overview. In Liquid Membranes: Theory and Applications; American Chemical Society: Washington, DC, 1987.

[5] Y. Inoue, Mechanistic principles of liquid membrane transport. In Liquid Membranes: Chemical Applications; Araki, T., Tsukube, H., Eds.; CRC Press: Boca Raton, FL, 1990.

[6] Schultz, J. S. Carrier-Mediated Transport in Liquid-Liquid Membrane Systems. In Recent Developments in Separation Science; Li, N. N., Ed.; CRC Press: Boca Raton, FL, 1977; Vol. IIIB.

[7] J. D. Goddard, J. S. Schultz, S. R. Suchdeo, Facilitated transport via carrier-mediated diffusion in membranes: Part II: mathematical aspects and analyses. *AIChE J.* **20** (1974) 625.

[8] J. D. Goddard, Further applications of carrier-mediated transport theory-A survey. *Chem. Eng. Sci.* **32** (1977) 795.

[9] A. Alhusseini, A. Ajbar, Mass transfer in supported liquid membranes: a rigorous model. *Mathematical and Computer Modelling* **32** (2000) 465–480.

[10] P. R. Danesi, E. P. Horwitz, G. F. Vandegrift, R. Chiarizia, Mass transfer rate through liquid membranes: Interfacial chemical reactions and diffusion as simultaneous permeability controlling factors. *Sep. Sci. Technol.* **16** (1981) 201.

[11] F.J. Alguacil, A.G. Coedo, M.T. Dorado, I. Padilla, Phosphine oxide mediated transport: modelling of mass transfer in supported liquid membrane transport of gold(III) using Cyanex 923. *Chem. Eng. Sci.* **56** (2001) 3115– 3122.

[12] L. Hernandez-Cruz, G. T. Lapidus, F. Carrillo-Romo, Modelling of nickel permeation through a supported liquid membrane. *Hydrometallurgy* **48** (1998) 265.

[13] A. Sastre, A. Madi, J.L. Cortina, N. Miralles, Modelling of mass transfer in facilitated supported liquid membrane transport of gold(III) using Phospholene derivatives as carriers. *J. Membr. Sci.* **139** (1998) 57– 65.

[14] J. Marchese, M.E. Campderros, A. Acosta, Mechanistic study of cobalt, nickel and copper transfer across a supported liquid membrane. *J. Cem. Technol. Biotechnol.* **57** (1993) 37– 42.

[15] Ting-Chia, Huang, Ruey-Shin, Juang,. Rate and mechanism of divalent metal transport through supported liquid membrane containing di-(2-ethylhexyl) phosphoric acid as a mobile carrier. *J. Cem. Technol. Biotechnol.* **42** (1998) 3– 17.

[16] J. Ruey-Shin, C. Juin-Dong, H. Huey-Chung, Dispersionfree membrane extraction: case studies of metal ion and organic acid extraction. *J. Membr. Sci.* **165** (2000) 59–73.

[17] P.J. Harrington, G.V. Stevens, Steady-state mass transfer and modelling in hollow fibre liquid membranes. *J. Membr. Sci.* **192** (2001) 83– 98.

[18] F.J. Alguacil, P. Navarro, Permeation of cadmium through a supported liquid membrane impregnated with Cyanex 923. *Hydrometallurgy* **61** (2001) 137– 142.

[19] L. Hernandez-Cruz, G.T. Lapidus, F. Carrillo-Romo, Modelling of nickel permeation through a supported liquid membrane. *Hydrometallurgy* **48** (1998) 265– 276.

[20] Bromberg, L.; Levin, G.; Libman, J.; Shanzer, A. A novel tetradentate hydromate as ion carrier in liquid membranes. *J. Membr. Sci.* **69** (1992) 143.

[21] Bromberg, L.; Lewin, I.; Warshawsky, A. Membrane extraction of mercury(II) and silver(I) by bis(di(2-ethylhexyloxy)thiophosphoryl) disulfide. *Hydrometallurgy* **33** (1993) 59.

[22] Akiba, K.; Ito, M.; Nakamura, S. Selective transport of yttrium (III) in the presence of iron(III) through liquid-membrane impregnating acidic organophosphonate mobile carrier. *J. Membr. Sci.* **129** (1997) 9.

[23] Chiarizia, R.; Horwitz, E. P.; Rickert, P. G.; Hodgson, K. M. Application of supported liquid membranes for removal of uranium from groundwater. *Sep. Sci. Technol.* **25** (1990) 1571.

[24] Chaudry, M. A.; Ahmed, B. Supported liquid membrane extraction study of (MoO4)2- ions using tri-n-octylamine as carrier. *Sep. Sci. Technol.* **27** (1992)1125.

[25] Chaudry, M. A.; Malik, M. T.; Ahmad, M. Transport of titanium- (IV) ions across di-2-ethylhexylphosphoric acid-CCl4 supported liquid membranes. *J. Radioanal. Nucl. Chem.* **157** (1992) 143.

[26] Chaudry, M. A.; Malik, M. T.; Ali, A. Transport of Mo(VI) ions through tri-n-octylamine-xylene based supported liquid membranes. Sep. Sci. Technol. **25** (1990) 263.

[27] Cox, J. A.; Bhatnagar, A. Analytical utility of coupled transport across a supported liquid membrane. Selective preconcentration of zinc. *Talanta* **32** (1990) 1037.

[28] Dozol, J. F.; Casas, J.; Sastre, A. M. Transport of cesium from reprocessing concentrate solutions through flat-sheet-supported liquid membranes: influence of the extractant. *Sep. Sci. Technol.* **30** (1995) 435.

[29] Fu, J.; Nakamura, S.; Akiba, K. Transport of palladium(II) through trioctylamine liquid membrane. *Sep. Sci. Technol.* **30** (1995) 793.

[30] Juang, R.; Liang, J. The competitive permeation of cobalt and nickel with supported liquid membranes. *Chem. Eng. Commun.* **126** (1993) 13.

[31] Juang, R.; Lo, R. Mass-transfer characteristics of a membrane permeation cell and its application to the kinetic studies of solvent extraction. *Ind. Eng. Chem. Res.* **33** (1994) 1001.

[32] Huang, T.; Tsai, T. Separation of cobalt and nickel ions in sulfate solutions by liquid-liquid extraction and supported liquid membrane with di(2-ethylhexyl)phosphoric acid dissolved in kerosene. *J. Chem. Eng. Jpn.* **24** (1991) 126.

[33] Marchese, J.; Campderros, M. E.; Acosta, A. Mechanistic study of cobalt, nickel and copper transfer across a supported liquid membrane. *J. Chem. Technol. Biotechnol.*, **57** (1993) 37.

[34] Molinari, R.; Drioli, E.; Pantano, G. Stability and effect of diluents in supported liquid membranes for Cr(III), Cr(VI), and Cd(II) recovery. *Sep. Sci. Technol.*, 24 (1989) 1032.

[35] Mohapatra, R.; Kanungo, S. B. Kinetics of Mn(II) from aqueous sulfate solution through a supported liquid membrane containing di(2-ethylhexyl)phosphoric acid in kerosene. *Sep. Sci. Technol.* **27** (1992) 1759.

[36] Nair, S. G.; Hwang, S. Selective transport of calcium ion from a mixed cation solution through an HDEHP/n-dodecane supported liquid membrane. *J. Membr. Sci.*, **64** (1991) 69.

[37] Noguerol, J.; Palet, C.; Valiente, M. Transport of selenite through a solid supported liquid membrane using sodium diethyldithiocarbamate, Na(DDTC), as carrier between hydrochloric acid solutions. *J. Membr. Sci.* **134** (1997) 261.

[38] Takigawa, D. Y. The effect of porous support composition and operating parameters on the performance of supported liquid membranes. *Sep. Sci. Technol.* **27** (1992) 325.

[39] Youn, I. J.; Lee, Y.; Lee, W. H. Analysis of permeation rate of cobalt ions across a supported liquid membrane containing HEH- (EHP). *J. Membr. Sci.* **100** (1995) 69.

[40] Saito, T. Deterioration of liquid membrane and its improvement in permeation transport of Zn(II) ion through a supported liquid membrane containing a bathocuproine. *Sep. Sci. Technol.* **27** (1992) 1.

[41] Saito, T. Selective transport of alkali and alkaline earth metallic ions through a supported liquid membrane containing tripentyl phosphate as a carrier. *Sep. Sci. Technol.* **28** (1993) 1629.

[42] Saito, T. Transport of cadmium(II) ion through a supported liquid membrane containing a bathocuproine. *Sep. Sci. Technol.* **26** (1991) 1495.

[43] Ikeda, I.; Yamazaki, H.; Konishi, T.; Okahara, M. Transport of mercury(II) through impregnated polybutadiene-o-nitrophenyl octyl ether membrane. *J. Membr. Sci.* **46** (1989) 113.

[44] Okushita, H.; Shimidzu, T. Membrane separation of Ga^{3+} by selective interaction of Ga^{3+} with N-octadecanoyl-N-phenylhydroxylamine. *J. Membr. Sci.* **116** (1996) 61.

[45] Szpakowska, M.; Nagy, O. B. Stability of supported liquid membranes containing Acorga P-50 as carrier. *J. Membr. Sci.* **129** (1997) 251.

[46] Kralj, D.; Breembroek, G. R. M.; Witkamp, G. J.; van Rosmalen, G. M.; Brecevic, L. Selective dissolution of copper oxalate using supported liquid membranes. *Solvent Extr. Ion Exch.* **14** (1996) 705.

[47] Yoshizuka, K.; Yasukawa, R.; Koba, M.; Inoue, K. Diffusion model accompanied with aqueous homogeneous reaction in hollow fiber membrane extractor. *J. Chem. Eng. Jpn.* **28** (1995) 59.

[48] Zha, F. F.; Fane, A. G.; Fell, C. J. D. Instability mechanisms of supported liquid membranes in phenol transport process. J. Membr. Sci. **107** (1995) 59.

[49] Zha, F. F.; Fell, C. J. D. Effect of surface tension gradients on stability of supported liquid membranes. *J. Membrane Sci.* **107**(1995) 75.

[50] W.R. Everest, S. Malloy, A design/build approach to deep aquifer membrane treatment in Southern California. *Desalination* **132** (2000) 41–45.

[51] P. Fu, H. Ruiz, J. Lozier, K. Thompson, C. Spangenberg, A pilot study on groundwater natural organics removal by low-pressure membranes. *Desalination* **102** (1995) 47–56.

[52] A. Gaid, G. Bablon, G. Turner, J. Franchet, J.C. Protais, Performance of 3 years' operation of nanofiltration plants. *Desalination* **117** (1998) 149–158.

[53] K. Glucina, A. Alvarez, J.M. Laine, Assessment of an integrated membrane system for surface water treatment. *Desalination* **132** (2000) 73–82.

[54] A.M. Hassan, A.M. Farooque, A.T.M. Jamaluddin, Al-Amoudi, A.S. Al-Sofi, M.A., A.F. Al-Rubaian, N.M. Kither, I.A.R. Al-Tisan, A. Rowaili, A demonstration plant based on the new NF-SWRO process. *Desalination* **131** (2000) 157–171.

[55] J.G. Jacangelo, R.R. Trussell, M. Watson, Role of membrane technology in drinking water treatment in the United States. *Desalination* **113** (1997) 119–127.

[56] R. Kettunen, P. Keskitalo, Combination of membrane technology and limestone filtration to control drinking water quality. *Desalination* **131** (2000) 271–283.

[57] A. Khalik, V.S. Praptowidodo, Nanofiltration for drinking water production from deep well water. *Desalination* **132** (2000) 287–292.

[58] K. Kosutic, B. Kunst, Removal of organics from aqueous solutions by commercial RO and NF membranes of characterized porosities. *Desalination* **142** (2002) 47–56.

[59] P. Laurent, P. Servais, D. Gatel, G. Randon, P. Bonne, J. Cavard, Microbiological quality before and after nanofiltration. *J. AWWA* **91** (1999) 62–72.

[60] B.B. Levine, K. Madireddi, V. Lazarova, M.K. Stentrom, M. Suffet, Treatment of trace organic compounds by membrane processes: at the Lake Arrowhead water reuse pilot plant. *Water Sci. Technol.* **40** (1999) 293–301.

[61] K. Madireddi, R.W. Babcock, B. Levine, T.L. Huo, E. Khan, Q.F. Ye, J.B. Neethling, I.H. Suffet, M.K. Stenstrom, Wastewater reclamation at Lake Arrowhead, California: an overview. *Water Environ. Res.* **69** (1997) 350–362.

[62] T. Matsuura, Progress in membrane science and technology for seawater desalination—a review. *Desalination* **134** (2001) 47–54.

[63] L.A. Mulford, J.S. Taylor, D.M. Nickerson, S.S. Chen, NF performance at full and pilot scale. *J. AWWA* **91** (1999) 64–75.

[64] H. Niemi, S. Palosaari, Calculation of the permeate flux and rejection in simulation of ultrafiltration and reverse osmosis processes. *J. Membr. Sci.* **84** (1993) 123–137.

[65] J.I. Oh, K. Yamamoto, H. Kitawaki, S. Nakao, T. Sugawara, M.M. Rahman, M.H. Rahman, Application of low-pressure nanofiltration coupled with a bicycle pump for the treatment of arsenic-contaminated groundwater. *Desalination* **132** (2000) 307–314.

[66] M. Otaki, K. Yano, S. Ohgaki, Virus removal in a membrane separation process. *Water Sci. Technol.* **37** (1998) 107–116.

[67] H. Ozaki, K. Sharma, W. Saktaywin, D. Wang, Y. Yu, Application of ultra low pressure reverse osmosis (ULPRO) membrane to water and wastewater. *Water Sci. Technol.* **42** (2000) 123–135.

[68] A.G. Pervov, E.V. Dudkin, O.A. Sidorenko, V.V. Antipov, S.A. Khakhanov, R.I. Makarov, RO and NF membrane systems for drinking water production and their maintenance techniques. *Desalination* **132** (2000) 315–321.

[69] O. Raff, R.D. Wilken, Removal of dissolved uranium by nanofiltration. *Desalination* **122** (1999) 147–150.

[70] C. Ratanatamskul, Description of behavior in rejection of pollutants in ultra low pressure nanofiltration. *Water Sci Technol.* **38** (1998) 453–462.

[71] J.A. Redondo, F. Lanari, Membrane selection and design considerations for meeting European potable water requirements based on different feedwater conditions. *Desalination* **113** (1997) 309–323.

[72] J. Schaep, B. Van der Bruggen, C. Vandecasteele, D. Wilms, Influence of ion size and charge in nanofiltration. *Separ. Purif. Technol.* **14** (1998) 155–162.

[73] J. Schaep, B. Van der Bruggen, S. Uytterhoeven, R. Croux, C. Vandecasteele, D. Wilms, E. Van Houtte, F. Vanlerberghe, Removal of hardness from groundwater by nanofiltration. *Desalination* **119** (1998) 295–302.

[74] B.M. Schneider, 1994. Membranes—Part 1—Nanofiltration compared to other oftening processes. Ultrapure Water 65.

[75] A. Seidel, J.J. Waypa, M. Elimech, Role of charge (Donnan) exclusion in removal of arsenic from water by a negatively charged porous nanofiltration membrane. *Environ. Eng. Sci.* **18** (2001) 105–113.

[76] R. Semiat, Desalination: present and future. *Water Int.* 25 (2000) 54–65.

[77] H.D.M. Sombekke, D.K. Voorhoeve, P. Hiemstra, Environmental impact assessment of groundwater treatment with nanofiltration. *Desalination* **113** (1997) 293–296.

[78] J.S. Taylor, L.A. Mulford, S.S. Chen, J.A.M. Hofman, 1995. Membrane filtration of pesticides. Proceedings of the Annual Conference AWWA 593.

[79] T.A. Tuhkanen, T.K. Kainulainen, T.K. Vartiainen, P.J. Kalliokoski, The effect of preozonization, ozone hydrogen-peroxide treatment, and nanofiltration on the removal of organic-matter from drinking-water. *Ozone-Science and Engineering* **16** (1994) 367–383.

[80] T. Urase, K. Yamamoto, S. Ohgaki, Effect of pore structure of membranes and module configuration on virus retention. *J. Membr. Sci.* **115** (1996) 21–29.

[81] T. Urase, J. Oh, K. Yamamoto, Effect of pH on rejection of different species of arsenic by nanofiltration. *Desalination* **117** (1998) 11–18.

[82] B. Van der Bruggen, J. Schaep, W. Maes, D. Wilms, C. Vandecasteele, Nanofiltration as a treatment method for the removal of pesticides from ground waters. *Desalination* **117** (1998) 139–147.

[83] B. Van der Bruggen, J. Schaep, D. Wilms, C. Vandecasteele, Influence of molecular size, polarity and charge on the retention of organic molecules by nanofiltration. *J. Membr. Sci.* **156** (1999) 29–41.

[84] B. Van der Bruggen, J. Schaep, C. Vandecasteele, D. Wilms, A comparison of models to describe the maximal retention of organic molecules. *Separ. Sci. Technol.* **35** (2000) 169–182.

[85] B. Van der Bruggen, C. Vandecasteele, Modelling of the retention of uncharged molecules with nanofiltration. *Water Res.* **36** (2002) 1360–1368.

[86] C. Ventresque, G. Bablon, The integrated nanofiltration system of the Mery-sur-Oise surface treatment plant (37 mgd). *Desalination* **113** (1997) 263–266.

[87] C. Ventresque, G. Turner, G. Bablon, Nanofiltration: from prototype to full scale. *J. AWWA* **89** (1997) 65–76.

[88] A. Waniek, M. Bodzek, K. Konieczny, Trihalomethanes removal from water using membrane processes. *Polish J. Environ. Studies* **11** (2002) 171–178.

[89] J.G. Wijmans, R.W. Baker, The solution-diffusion model: a review. *J. Membr. Sci.* **107** (1995) 1–21.

[90] E. Wittmann, P. Cote, C. Medici, J. Leech, A.G. Turner, Treatment of a hard borehole water containing low levels of pesticide by nanofiltration. *Desalination* **119** (1998) 347–352.

[91] M.T. Yahya, C.B. Bluff, C.P. Gerba, Virus removal by slow sand filtration and nanofiltration. *Water Sci. Technol.* **27** (1993) 445–448.

[92] H.H. Yeh, I.C. Tseng, S.J. Kao, W.L. Lai, J.J. Chen, G.T. Wang, S.H. Lin, Comparison of the finished water quality among an integrated membrane process, conventional and other advanced treatment processes. *Desalination* **131** (2000) 237–244.

[93] P. Eugene, M. B. Stanley, Oil/water separation using nanofiltration membrane technology, *Sep. Sci. Technol.***36** (2001) 1527–1542.

[94] R.A. Bergman, Membrane softening versus lime softening in Florida—a cost comparison update. *Desalination* **102** (1995) 11–24.

[95] P. Fu, H. Ruiz, K. Thompson, C. Spangenberg, Selecting membranes for removing NOMand DBP precursors. *J. AWWA* **86** (1994) 55–72.

[96] T. Lo, R.G. Sudak, Removing color from a groundwater source. *J. AWWA* **84** (1992) 79–87.

[97] B.M. Watson, C.D. Hornburg, Low-energy membrane nanofiltration for removal of color, organics and hardness from drinking- water supplies. *Desalination* **72** (1989) 11-22.

[98] J.S. Taylor, D.M. Thompson, J.K. Carswell, Applying membrane processes to groundwater sources for trihalomethane precursor control. *J. AWWA* **79** (1987) 72–82.

[99] B. Van der Bruggen, K. Everaert, D. Wilms, C. Vandecasteele, The use of nanofiltration for the removal of pesticides from ground water: an evaluation. *Water Sci. Technol.: Water Supply* **1** (2001) 99–106.

[100] P. Berg, G. Hagmeyer, R. Gimbel, Removal of pesticides and other micropollutants by nanofiltration. *Desalination* **113** (1997) 205–208.

[101] P. Berg, R. Gimbel, 1997. Rejection of trace organics by nanofiltration. Membrane Technology Conference, AWWA, New Orleans.

[102] Y. Kiso, Y. Nishimura, T. Kitao, K. Nishimura, Rejection properties of non-phenylic pesticides with nanofiltration membranes. *J. Membr. Sci.* **171** (2000) 229–237.

[103] J.A.M.H. Hofman, E.F. Beerendonk, H.C. Folmer, J.C. Kruithof, 1997. Removal of pesticides and other micropollutants with cellulose- acetate, polyamide and ultra low pressure reverse osmosis membranes—'The next generation….', Workshop on Membranes in Drinking Water Production—Technical Innovations and Health Aspects, L'Aquila, Italy.

[104] T. Montovay, M. Assenmacher, F.H. Frimmel, Elimination of pesticides from aqueous solution by nanofiltration. *Magyar Kemiai Folyoirat* **102** (1996) 241–247.

[105] E.O. Kartinen, C.J. Martin, An overview of arsenic removal processes. *Desalination* **103** (1995) 79–88.

[106] J.J. Waypa, M. Elimelech, J.G. Hering, Arsenic removal by RO and NF membranes. *J. AWWA* **89** (1997) 102–114.

3. CHAPTER THREE

EXPLORASTION OF HEAVY METAL IONS TRANSMEMBRANE FLUX ENHANCEMENT ACROSS A SUPPORTED LIQUID MEMBRANE BY APPROPRIATE CARRIER SELECTION

3.1 Introduction

The supported liquid membranes (SLM) technique has received considerable attention over the past few decades because they offer a lot of advantages over conventional separation technologies, such as easy operation, low capital and operating costs, low energy consumption, continuous operation, high selectivity, relatively high fluxes, combination of extraction, stripping and regeneration processes into a single stage, uphill transport against concentration gradients, and small usage of amounts of extractants [1-5]. SLM has been demonstrated as an effective tool for the selective separation and recovery of resources from dilute solutions, particularly for the removal and recovery of toxic metals, e.g. cadmium or copper ions, from waste effluents [6].

Transport of metal species through a supported liquid membrane involves a continuous recycle of the following processes: (1) metal complexation with the carrier; (2) the complex traveling from the feed/membrane interface to the membrane/stripping interface; (3) decomplexation and partition of metal species into the stripping phase; (4) the decomplexed carrier traveling back to the membrane/feed interface where it again complexes with the metal species [3]. The steps involving the complexation reactions are

very crucial. The structure and nature of organic carriers present in the membrane probably play a decisive role in determining the effectiveness of the extraction step. Therefore, the choice of suitable carriers is vital to obtain a high performance SLM.

In past decades, various carriers for the separation of cadmium, the highly toxic metal ion, using SLM systems have been intensively examined for different experimental conditions [7-13]. However, to our best knowledge, no work has been done to theoretically predict the extraction power of carriers for Cd(II) in SLM systems. In this work, a reliable theoretical prediction based on quantum chemical computation has been proposed for the carrier selection based on the extraction process in a SLM system for Cd(II) removal, a typical and practically important example. The computational work can reduce the tedious laboratory experiments significantly and provide guidance when choosing an effective carrier for SLM systems.

The quaternary ammonium salts Aliquat 336, hydroxyquinoline Kelex 100 have been proven to be effective extractants for Cd(II) and β-diketone LIX54 is also a possible extraction candidate for Cd(II) [10, 14, 15, 16]. The quaternary ammonium salts Aliquat 336, hydroxyquinoline Kelex 100 and β-diketone LIX54 have different functional groups for complexation with Cd(II) [10, 14, 15, 16], resulting different extraction mechanisms with Cd(II). Therefore, they have been specifically chosen as the carrier candidates for Cd (II) removal through the SLM system in this work. Both experimental and computational results reveal Aliquat 336 is the best one. Subsequently, the systematic studies for Aliquat 336/Cd(II), with respects to the Cd(II) flux as a function of carrier

concentration, hydrodynamic conditions, stripping phase compositions, feed concentrations and anion additions in the feed were carried out.

3.2 Experimental Section

The quaternary ammonium salts Aliquat 336, hydroxyquinoline Kelex 100, β-diketone LIX54 were diluted in kerosene and used as the carriers in the liquid membrane phase. Cadmium (II) solutions were used as the feed phases by dissolving $CdCl_2 \cdot H_2O$ in 1M HCl or deionized water. Hydrochloric acid, Ammonium acetate and ethylenediaminetetraacetic acid (EDTA) were employed as stripping phases in the SLM systems. A Whatman® PTFE membrane filter (England) was utilized as a membrane support, having a diameter of 4.7 cm and a thickness of 150 μm with ~80% porosity and an average pore size of 0.2 μm. The impregnated membrane after being blotted with a soft paper sheet to remove the extra oil was then placed in a cell holder of the SLM system. The SLM system had two Teflon® chambers holding the feed and strip solutions with volume of 37 ml each and the effective membrane surface area was 8.7 cm^2. Both aqueous phases were mechanically stirred with Teflon® impellers in connection with an overhead mixer.

Metal concentrations in the stripping phase were measured by a Perkin Elmer Optima 3000 ICP-AES (Norwalk, CT). Membrane fluxes were determined by monitoring metal concentration in the stripping phase as the function of time based on the following equation:

$$J = \frac{dC_s}{dt}\frac{V}{S} \tag{3.1}$$

where V is the volume of the stripping phase; S is the effective surface area of the membrane; C_s is the molar concentration of metal in the stripping phase and t is the time elapsed.

Carriers and their complexes formed after reaction with 10mM $CdCl_2$ in 1M HCl (for Aliquat 336) or 10mM $CdCl_2$ only (for the other two carriers) were analyzed by a Bio-Red FTS135 FT-IR spectrometer to study the reaction mechanisms of the carriers with cadmium species. For readers' information, $CdCl_2$ in the concentrated HCl solution for Aliquat 336 extraction is because Aliquat 336, as an anion exchanger, only extracts $CdCl_4^{2-}$, an effective component in the aqueous solution [16].

In order to investigate the effect of sulfate and nitrate anions on cadmium flux, various amounts of sodium sulfate or sodium nitrate were added into the feed phase containing cadmium chloride and hydrochloric acid at 10mM and 1M, respectively. The concentrations of sulphate and nitrate in the aqueous phase were analyzed by using an ion chromatograph (Metrohm Model 702) equipped with a conductivity detector and a Hamilton PRP-X 100 anion column was used. It was operated at a flow rate of 2 ml/min with an eluent containing 1.7 mM $NaHCO_3$ and 1.8 mM Na_2CO_3.

3.3 Computational Methodology

Calculation and simulation for solving problems in chemical engineering are found to give reliable results [17-19], especially quantum chemical computations which are an increasingly important tool in chemical science and engineering. They are good approaches to theoretically select effective SLM carriers by providing the molecular structure-property relations, which is the key to bridge the relation of the carrier structures with their extractabilities. It is well known that for the organometallic compounds such as the cadmium-carrier complexes, density functional theory calculations generally perform well [20]. Therefore, the reaction processes of Cd (II) with these three carriers were analyzed with the first-principles density functional theory calculations. In the current work, quantum chemical computations were achieved based on the following procedure. Firstly, in order to obtain good initial coordinates for density functional theory optimization, the geometries of the carriers and cadmium-carrier complexes were mechanically minimized with the general Amber force field by using AMBER 8 [21]. Secondly, optimizations of the geometries of the carriers and the cadmium-carrier complexes were achieved with Becke's three-parameter hybrid functional coupled with the Lee-Yang-Parr correlation functional (B3LYP) level of theory at 3-21g basis set. The split-valence basis set 3-21g used here means that the inner shell orbitals are represented by three Gaussians, and the valence orbitals by two Gaussians for the first Slater type orbital (STO) and by one Gaussian for the second STO. Thirdly, the single point energies of the fully optimized geometries of the carriers and the cadmium-carrier complexes were calculated using B3LYP at the 3-21g basis set. All the first-principles density functional theory optimizations were performed with the GAUSSIAN 03 program suite [22]. Finally, the energy changes in complex formation

processes were calculated by $\Delta E = \Sigma E_{\text{Products}} - \Sigma E_{\text{Reactants}}$. The links between the quantum computation results and the extraction capabilities of the carriers are as follows: generally, the more negative energy change for the carrier/Cd(II) system, the more favorable process for the formation of the complex and consequently the better the extraction capability of the carrier.

3.4 Results and Discussion

3.4.1 Quantum Chemical Calculation Results

The optimized Aliquat 336/Cd(II) geometry (Figure 3.1A) shows the tetrahedral $CdCl_4^{2-}$ is surrounded by two NR_4^+ species, with the same distances between cadmium and two nitrogen atoms. In the Kelex 100/Cd(II) complex (Figure 3.1B), Cd^{2+} as a magnetic nuclear center is surrounded by a trapezoid arrangement of two oxygen ligands and two nitrogen ligands, with different distances between Cd-O and Cd-N. From the optimized LIX54/Cd(II) geometries (Figure 3.1C), Cd^{2+} as a center is surrounded by a square planar arrangement of four oxygen ligands with all the same distances between cadmium and four oxygen atoms.

The single point energy calculation results show that the energy changes in the complex formation process are in the order of Aliquat 336/Cd(II) > Kelex 100/Cd(II) > LIX 54/Cd(II), with energy changes of -657.79, -329.19 and 96.32 kcal/mol, respectively.
The computational results reveal that Aliquat 336 is the best carrier for cadmium extraction followed by Kelex 100 and LIX54 is not suitable for Cd(II) extraction.

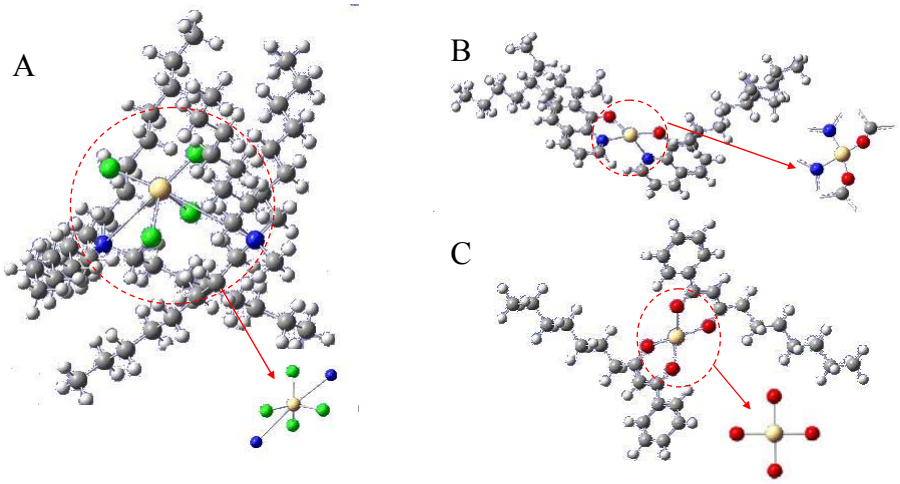

Figure 3.1 Optimized geometries of carrier/Cd (II) complexes. (A) Aliquat 336/Cd (II) complex. Energy change: -657.79 kcal/mol; distances of Cd-Cl are 2.55, 2.55, 2.58, 2.61 Å; distances of Cd-N are 4.98 and 5.11Å. (B) Kelex 100/Cd (II) complex. Energy change:-329.19 kcal/mol; distances of Cd-N are 2.26 and 2.29Å; distances of Cd-O are 2.16 and 2.15 Å. (C) LIX54/ Cd (II) complex. Energy change: 96.32 kcal/mol; distances of Cd-O are all 2.16 Å.

3.4.2 Formation of Cadmium Complexes with Carriers

The active components of Aliquat 336, Kelex 100 and LIX 54 are tri-*n*-octylmethylammonium chloride, 7-(4-ethyl-l-methyloctyl)-8-hydroxyquinoline and 1-phenyl-1, 3-decanedione, respectively. The general reaction mechanisms involving Aliquat 336/Cd(II), Kelex 100/Cd^{2+} and LIX 54/Cd^{2+} complexes are described in the following expressions:

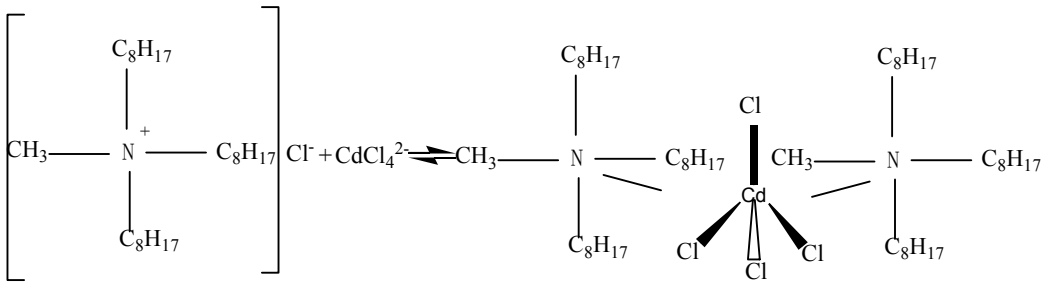

(3.2)

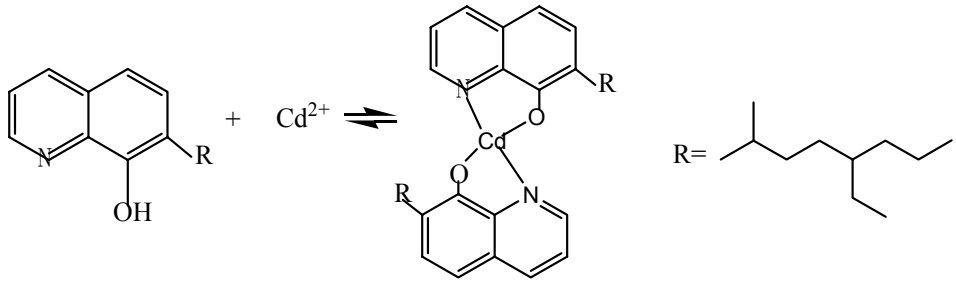

(3.3)

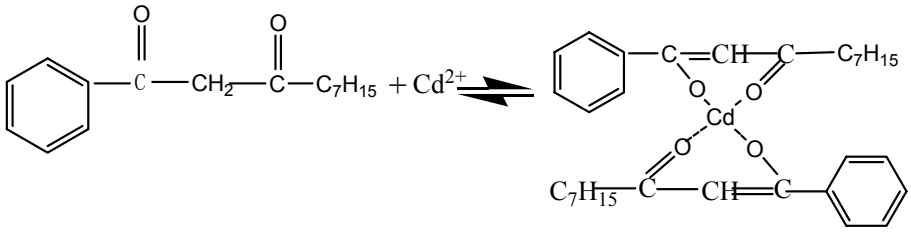

(3.4)

Figure 3.2 shows the IR spectra of carriers and their complexes after reaction with cadmium (II). The spectrum of the Aliquat 336 agrees with reference [23]. The spectra of both Aliquat 336 and Aliquat 336/Cd(II) complex have the strong peaks around 2970~2860 cm^{-1}, 1150~1092cm^{-1} and 725cm^{-1}, which are the characteristic peaks of the -CH_3 group, C-N symmetric stretching vibration and -$[CH_2]_n$- group, respectively [24, 25]. The bands observed at 3500 ~3360cm^{-1} is assigned to the N-Cl stretching vibration. It shifts to the region 3530~3390cm^{-1} in the case of Aliquat 336/Cd (II) complex, probably due to the coordination of quaternary N with Cd^{2+}. Cd-Cl vibrations of the four–coordinated approximately tetrahedral species $CdCl_4^{2-}$ could not be identified, which

surely lie in the spectral range below 400 cm^{-1} as observed in some other similar complexes [26, 27].

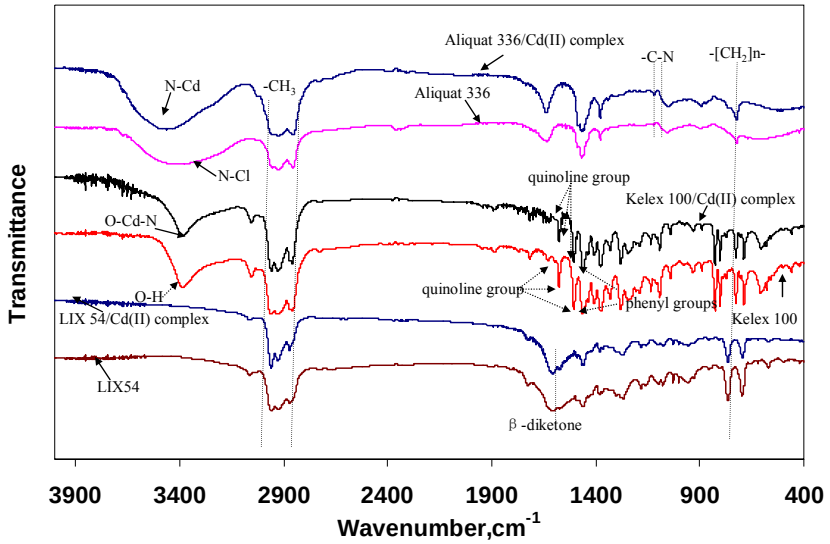

Figure 3.2. FTIR spectra of carriers and their complexes with cadmium (II).

For the FTIR spectra of Kelex 100 and Kelex 100/Cd^{2+}, both spectra have peaks at 1628, 1578 and 1500 cm^{-1}, which are the characteristic peaks of quinoline group [28]. The bands observed at 1500 and 1463 cm^{-1} involve a C-C/C-N stretching and C-H bending vibration associated with the pyridyl and phenyl groups. The bands recorded in the IR spectra contain absorption bands with peak positions at 1280, 1238 and 1113 cm^{-1}, mainly originating from a C-H/C-C-N bending and C-N stretching vibrations [29]. There is a strong peak at 3394 cm^{-1} from O-H stretching vibration of Kelex 100 which shifting to 3391 cm^{-1} due to the coordination of O and N with Cd^{2+} since the coordination of the carrier with cadmium(II) results in the reduction of electron cloud and force constant, leading to a red shift of the absorption frequency [30].

The spectra of LIX 54 and the loaded organic phases are very similar and exhibit the main characteristic vibrational modes of LIX 54. This indicates that the non-extractability or low-extractability of LIX54 for cadmium species, agreeing well with the quantum chemical computational results.

3.4.3 Influence of the Carrier Concentration on Cadmium Flux

To determine the influence of the carriers' concentrations on cadmium transport, their concentrations from 10 v/v % to 90 v/v % in kerosene were used to impregnate the membrane filters. Figure 3.3 clearly shows that the best carrier is Aliquat 336 followed by Kelex 100 at the correspondingly same carrier concentrations and LIX 54 is not a suitable carrier for cadmium (II). This is exactly in accordance with our computational results, i.e. the order of energy changes for carrier/Cd(II) formation processes, indicating that the quantum chemical computation method is an effective tool for prediction of the carriers' extractabilities. Theoretically, the more negative energy change, the more favorable formation of the complex. In the treatment of industrial effluents, after consideration of the general reaction mechanisms involving carrier/heavy metal complexes, the energy changes in complex formation processes can be obtained via quantum chemical calculations. Carriers with more negative energy change can be selected for the specific heavy metal removal in the SLM systems. For example, from our calculation LIX54 is not a suitable carrier for cadmium removal from industrial effluents;

however, it is a good carrier for copper removal with energy change in LIX54/Cu (II) complex formation process at -99.33 kcal/mol [31].

As also can be seen from Figure 3.3, an increase in the carrier concentration results in an increase in the cadmium flux for all systems and flux reaches the maximum at a carrier concentration of 50 v/v % for Aliquat 336 and Kelex 100. Further increase in the cadmium removal rate is inhibited probably by the reduced cadmium-carrier diffusion coefficient in the membrane phase. The lower diffusion coefficient at higher carrier concentrations can be attributed to the increasing viscosity of the organic membrane phase [32]. In the subsequent systematically experimental studies, 50 v/v % of Aliquat 336 in kerosene was used as the membrane organic phase.

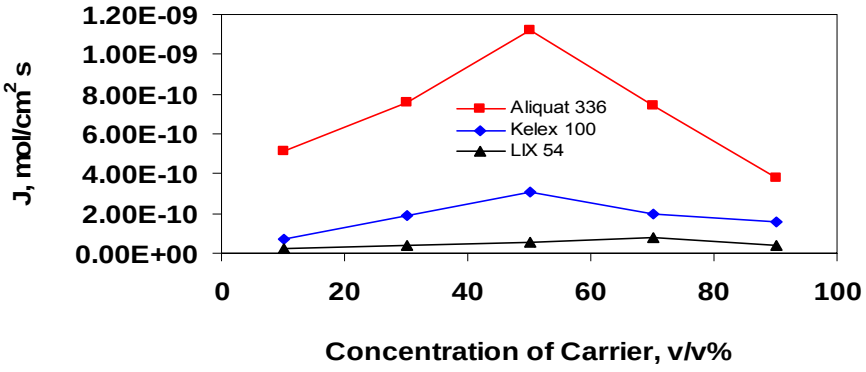

Figure 3.3 Influence of carrier concentration on cadmium flux. Source phase: 10mM $CdCl_2$ in 1M HCl for Aliquat 336, 10mM $CdCl_2$ for other carriers. Stripping phase: 1mM EDTA. Stirring rate: 400rpm.

Our investigation on the long-term stability of the SLM systems has shown that up to 250 hours' running (the feed solution replaced by fresh one every 24 hours), the flux of Cd(II) remains unchanged. This indicates the carrier stays stably in the SLM systems over a expanded period of time for Cd(II) removal process.

3.4.4 Influence of Stripping Phase Composition on the Transport of Cadmium (II)

Since extraction and stripping processes are integral parts of SLM systems, which work together for the continuous transport of cadmium (II), it is important to investigate the influence of stripping phase composition to obtain an efficient SLM system. A lot of strippants have been used for cadmium extraction. However, there has no attention been paid to EDTA (ethylenediaminetetraacetic acid). The fluxes for various strippants, including 1 mM HCl, 2 M HCl, 1 mM CH_3COONH_4 and 1 mM EDTA, are 4.00×10^{-11}, 6.00×10^{-11}, 5.90×10^{-10} and 1.12×10^{-9} mol/(cm^2·s), respectively. These results show the most effective strippant is 1 mM EDTA. The effectiveness of EDTA much higher than that of CH_3COONH_4 can be attributed to its higher stability constant of EDTA-Cd(II) complex at $10^{16.6}$ than that of CH_3COO^--Cd(II), $10^{12.6}$ [33]. Thus, 1mM EDTA was used as the stripping phase throughout the subsequent experiments conducted.

3.4.5 Influence of the Stirring Speed on Cadmium Flux

Stirring in both aqueous phases could provide homogeneous environments and reduce the mass transfer resistances in a SLM system. It is important to investigate the influence of the stirring rate on the cadmium flux in order to obtain a higher performance of SLM

system. This investigation has been studied with feed and strip conditions being maintained as: 10 mM Cd (II) in 1M HCl and 1 mM EDTA, respectively. Experiments at the same stirring rates for both aqueous phases at 100, 200, 400, 600 and 800 rpm were carried out, resulting in fluxes of 4.8×10^{-10}, 8.5×10^{-10}, 1.12×10^{-9}, 1.13×10^{-9}, 1.15×10^{-9} mol/(cm^2·s), respectively. This shows the flux increase from 100 to 400 rpm, and beyond that a virtually constant cadmium flux is obtained, indicating a minimum aqueous diffusion layer thickness and the correspondingly minimum resistances in both feed and strip unstirring layers are reached at 400rpm. It can be assumed that the resistances of the aqueous unstirring layers to the overall mass transfer process to be constant when stirring speed is larger than 400 rpm [34]. Thus a stirring rate of 400 rpm was maintained throughout the subsequent investigations.

3.4.6 Influence of Feed Cadmium (II) Concentration on Cadmium (II) Transport

The results concerning cadmium (II) flux from the feed phase containing various concentrations of cadmium (II) are shown in Figure 3.4. As can be seen from Figure 3.4, the cadmium (II) flux increases with feed concentration from 4×10^{-3} M to 10^{-2} M and then reaches a plateau, in the concentration range of 1.2×10^{-2} M-1.6×10^{-2} M. At lower feed concentrations, the increase of the cadmium (II) flux indicates that the diffusion of cadmium (II) in the stagnant aqueous layers is the rate-controlling step. At higher metal concentrations, the carrier on the feed side of the membrane in this case is saturated with cadmium and the transport is limited by the diffusion of cadmium-carrier complexes through the membrane [35].

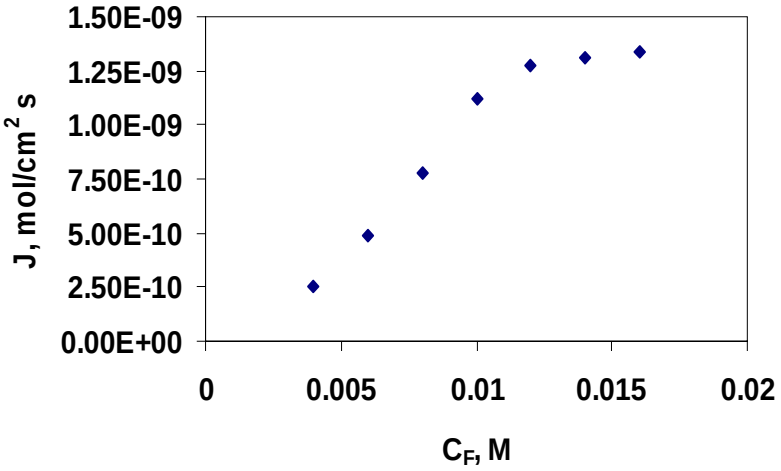

Figure 3.4 Influence of initial concentration of Cd (II) on metal flux. Stripping phase: 1mM EDTA. Carrier: 50 vol/vol % Aliquat 336. Stirring rate: 400rpm.

3.4.7 Influence of Sulfate and Nitrate on Cadmium Flux

Results from previous sections reveal that the SLM system has the highest performance with a cadmium flux of 1.12×10^{-9} mol/(cm^2·s) when the experimental conditions are as follows: membrane phase, 50 vol/vol % Aliquat 336 in a PTFE membrane; stripping phase, 1mM EDTA; stirring speed, 400rpm; feed phase, 10mM $CdCl_2$ in 1M HCl. In order to obtain a possible higher cadmium flux by introducing foreign anion and consequently propose a new method for the enhancement of metal ion flux, influence of additional anions in the feed solution on the cadmium flux has been studied.

To quantitatively determine influence of anion on the cadmium flux, we vary the concentration of additional sulfate and nitrate in the feed solution. The results are given in Figure 3.5A.

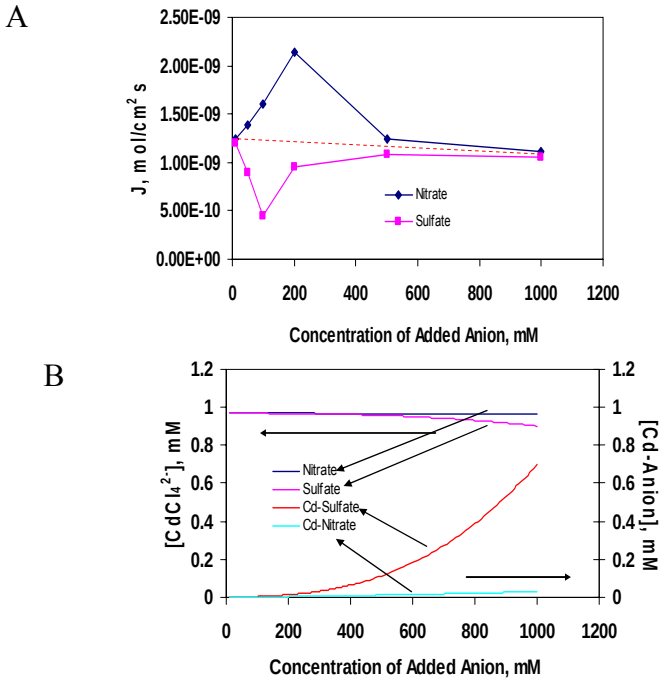

Figure 3.5 (A) Influence of concentration of added anion on metal flux. Stripping phase: 1mM EDTA. Feed solution: 10mM $CdCl_2$ in 1M HCl with various concentrations of salts. Carrier: 50 vol/vol % Aliquat 336. Stirring rate: 400rpm. (B) Influence of concentration of anions on the extractable $CdCl_4^{2-}$ species and the formed Cd-anion complex.

In order to understand the results in Figure 3.5A, we introduce the following mechanism described by Lamb et al. [36]:

$$mCd_F + nA_F = (Cd_mA_n)_M \tag{3.5}$$

$$(Cd_mA_n)_M + L_M = (Cd_mA_nL)_M \tag{3.6}$$

where Cd is cadmium cation, A is anion (sulfate, nitrate or chloride), Cd_mA_n is cation-anion pair, L is Aliquat 336, Cd_mA_nL is cadmium complex associated with anion.

Subscripts F and M indicate species in the feed and membrane phase, respectively. Eqns 3.5 and 3.6 are described by partition coefficient k and the equilibrium constant K, respectively.

In Lamb et al.'s work [36], they derived eq (3.7) to describe the Cd(II) transmembrane flux:

$$J_{Cd} = \frac{DkKC_L}{l}\left(\frac{Cd_F^2}{1+kKCd_F}\right) \tag{3.7}$$

where J_{Cd} is the cadmium flux, D is the diffusion coefficient of the complex Cd_mA_nL, l is the length of the diffusion path, Cd_F is the feed cadmium concentration and C_L is the carrier concentration in the membrane phase. The K is the thermodynamic equilibrium constant defined by the concentration of the cadmium-anion-carrier complex in the organic membrane phase divided by the product of cadmium-anion concentration and carrier concentration in the organic membrane phase.

From Eq. 3.7, we can identify that J_{Cd} increases as an increasing K and eventually levels off when K becomes very large. At very large K, $k{\cdot}K{\cdot}Cd_F >> 1$ in Eq. 3.7 holds, J_{cd} is independent of K; whereas at low K value and $k{\cdot}K{\cdot}Cd_F << 1$, Eq. 3.7 reduces to Eq 3. 8

$$J_{Cd} = \frac{DkKC_L Cd_F^2}{l} \tag{3.8}$$

Partition coefficient k is related to the Gibbs free energy of partitioning between water and membrane, ΔG_p, by the equation

$$\Delta G_p = -RT \ln k \tag{3.9}$$

Thus, eq 3.8 becomes

$$J_{Cd} = B \exp(-\Delta G_p / RT) \tag{3.10}$$

where $B=D \cdot K \cdot C_L \cdot Cd_F^2/l$

Furthermore,

$$\Delta G_p = \Delta G_p^{Cd} + \Delta G_p^{A} + \Delta G_p^{CdA} \tag{3.11}$$

where ΔG_p^{Cd}, ΔG_p^{A}, ΔG_p^{CdA} represent the free energies for partitioning of the Cd, anion and the interaction of the Cd with the anion within the membrane phase, respectively.

And ΔG_p^{A} can be expressed by the equation

$$\Delta G_p^{A} = \Delta G_{g \to M}^{A} - \Delta G_{g \to W}^{A} \tag{3.12}$$

where $\Delta G_{g \to M}^{A}$ and $\Delta G_{g \to W}^{A}$ are the free energies of transferring the anion from the gas phase to the membrane phase and that of the gas phase to water, respectively.

Thus eq 3.11 becomes

$$\Delta G_p = \Delta G_p^{Cd} + \Delta G_{g \to M}^{A} - \Delta G_{g \to W}^{A} + \Delta G_p^{CdA} \tag{3.13}$$

Combining eqs 3.10 with 3.13, we can get

$$\ln J_{Cd} = (F + \Delta G_{g \to W}^{A}) / RT \tag{3.14}$$

where $F= RTlnB-\Delta G_p^{Cd}-\Delta G_{g \to M}^{A}-\Delta G_p^{CdA}$ and it can be assumed to be a constant [36].

From eq 3.14, it can be seen that J_{cd} is a function of $\Delta G_{g\rightarrow w}^{A}$. Values of $\Delta G_{g\rightarrow w}^{A}$ for sulfate, chloride and nitrate are -238.7, -75.8 and -69.5 kcal/mol, respectively [37, 38]. This may contribute to the fact that Cd fluxes with nitrate addition in the feed solution are always higher than control while the fluxes are always lower when sulfate anions are added. It was also reported by He et al. [9] that the cadmium flux was promoted by adding I^- ($\Delta G_{g\rightarrow w}^{A}$ at -61.4 kcal/mol) [37, 38] into the Cl^- contained feed solution.

As can be seen in Figure 3.5A, when $NaNO_3$ is at lower concentrations, from 0 to 200 mM, the Cd (II) flux increases gradually from 1.12×10^{-9} to 2.14×10^{-9} mol/(cm^2·s), i.e. by 91%. In this case the feed solution becomes a mixture of $CdNO_3$ with $CdCl_2$, which has a free energy of hydration between -75.8 and -69.5 kcal/mol, and the free energy of hydration of the mixture becomes less negative when the amount of $CdNO_3$ increases with more nitrate addition. Therefore cadmium flux increases gradually. Similarly, this is the reason for the decrease of cadmium flux at low Na_2SO_4 concentration stage. However, cadmium flux deceases gradually from 2.14×10^{-9} to 1.13×10^{-9} mol/(cm^2·s) when $NaNO_3$ concentration increases from 200mM to 1M. The decrease maybe due to the competition between NO_3^- and $CdCl_4^{2-}$ to react with the carrier in the membrane phase, leading to less carrier for $CdCl_4^{2-}$ extraction. This argument can also be supported by the presence of 12.8 ppm NO_3^- in the stripping solution after 5-hour experiment with initial addition of 1M $NaNO_3$ in the feed. On the other hand, when the concentration of Na_2SO_4 increases from 100mM to 1M, the flux increases due to the fact that the concentration of Cd-sulfate complex increases significantly as shown in Figure 3.5B. This leads to an increase in the amount of extraction of Cd-sulfate complex based on eq 3.6 and consequently enhances

the total flux of Cd(II) in view of only about 10% decrease of $CdCl_4^{2-}$ as the extractable form. It is worth noting that, in the case with higher feed sulfate concentrations, Cd(II) flux increases but cannot reach as high as that of the control one.

The effect of anion(s) addition into the feed plays an important role on the Cd(II) transmembrane flux through SLM system and holds significant implications. From our studies, an enhanced Cd(II) flux can be achieved by adding anion(s) with less negative free energy of hydration at appropriate concentrations.

3.5 Summary

1. Quantum chemical computation can be proposed for carrier selection in supported liquid membrane (SLM) systems for heavy metal ions removal. The single point energy calculation results show that the energy changes in the complex formation process are in the order of Aliquat 336/Cd(II) > Kelex 100/Cd(II) > LIX 54/Cd(II), with energy changes of -657.79, -329.19 and 96.32 kcal/mol, respectively. Generally, the more negative energy change for the carrier/Cd(II) system indicates the more favorable process for the formation of the complex and consequently the better the extraction capability of the carrier. The computational results of the energy changes for the carrier/Cd(II) system show that Aliquat 336 is the best carrier for cadmium extraction followed by Kelex 100 and LIX54 is not suitable for Cd(II) extraction.

2. In the supported liquid membrane systems, heavy metal transmembrane flux can be enhanced effectively (with a flux increase by 91% in our case) by adding only small amount of anion(s) with less negative free energy of hydration.

3. The optimal conditions in our investigated SLM system for Cd(II) removal are as follows: membrane phase, 50 vol/vol % Aliquat 336 in an impregnated PTFE membrane; stripping phase, 1mM EDTA; stirring speed, 400rpm.

References

(1) Sirkar, K.K. Membrane separation technologies: Current developments. *Chem. Eng. Commun*. 1997, 157, 145-184.

(2) Gumi, T.; Valiente, M.; Khulbe, K.C.; Palet, C.; Matsuura, T. Characterization of activated composite membranes by solute transport, contact angle measurement, AFM and ESR. *J. Membr. Sci.* 2003, 212, 123–134.

(3) Kocherginsky, N.M.; Yang, Q.; Lalitha, S. Recent advances in Supported Liquid Membrane technology. *Sep. Purif. Technol.* 2007, 53, 171-177.

(4) Di Luccio,M.; Smith, B.D.; Kida, T.; Borges, C. P. ; Alves, T. L. M. Separation of fructose from a mixture of sugars using supported liquid membranes. *J. Membr. Sci.* 2000, 174, 217-224.

(5) Cooper, C.A; Lin, Y.S.; Gonzalez, M. Spearation properties of surface modified silica supported liquid membrane for divalent metal removal/recovery. *J. Membr. Sci.*2004, 229, 11-25.

(6) Ndungu, K.; Hurst, M.P.; Bruland, K.W. Comparison of copper speciation in estuarine water measured using analytical voltammetry and supported liquid membrane techniques. *Environ. Sci. Technol.*2005,39, 3166-3175.

(7) He, D.S.; Ma, M. Kinetics of cadmium (II) transport through a liquid membrane containing tricapryl amine in xylene. *Sep. Sci. Technol.* 2000, 35, 1573-1585.

(8) Urtiaga, A.M. et al. Comparison of liquid membrane processes for the removal of cadmium from wet phosphoric acid. *J. Membr. Sci.* **2000**, 164, 229-240.

(9) He, D.S. et al. Transport of cadmium ions through a liquid membrane containing amine extractants as carriers. *J. Membr. Sci.* **2000**, 169, 53-59.

(10) Wang, L.J.; Paimin, R.; Cattrall, R.W.; Shen, W.; Kolev, S.D. The extraction of cadmium (II) and copper(II) from hydrochloric acid solutions using an Aliquat 336/PVC membrane. *J. Membr. Sci.* **2000**, 176, 105-111.

(11) Schimmel, K. A.; Ilias, S.; Akella, S. Nondispersive liquid-liquid extraction of Zn(II), Cu(II), Co(II) and Cd(II) from dilute solution with DEHPA in a hollow-fiber membrane module. *Sep. Sci. Technol.* **2001**, 36, 805-821.

(12) Nowier, H.G.; El-Said, N.; Aly, H.F. Carrier-mediated transport of toxic elements through liquid membranes-Transport of Cd(II) from high salinity chloride medium through supported liquid membrane containing TBP/cyclohexane. *J. Membr. Sci.* **2000**, 177, 41-47.

(13) Juang, R.S.; Kao, H.C.; Wu, W.H. Liquid membrane transport and separation of Zn^{2+} and Cd^{2+} from sulfate media using organophosphorus acids as mobile carriers. *J. Chem. Technol. Biotechnol.* **2004**, 79, 140-147.

(14) Mellah A. ; Benachour, D. Solvent extraction of heavy metals contained in phosphoric acid solutions by 7-(4-ethyl-1-methyloctyl)-8-hydroxyquinoline in kerosene diluent. *Hydrometallurgy* **2006** , 81, 100-103.

(15) Kyuchoukov, G.; Bogacki, M.B.; Szymanowski, J. Copper extraction from ammoniacal solutions with LIX 84 and LIX 54. *Ind. Eng. Chem. Res.* **1998**, 37, 4084-4089.

(16) Juang, R.S.; Kao, H.C.; Wu, W.H. Analysis of liquid membrane extraction of binary Zn (II) and Cd (II) from chloride media with Aliquat 336 based on thermodynamic equilibrium models. *J. Membr. Sci.* **2004**, 228, 169-177.

(17) Cao DP, Jiang T, Wu JZ. A hybrid method for predicting the microstructure of polymers with complex architecture: Combination of single-chain simulation with density functional theory. J. Phys. Chem. B 2006, 110, 21882-21889.

(18) Sun LX , Zhao HG , McCabe C . Predicting the phase epuilibria of petroleum fluids with the SAFT-VR approach. A.I.CHE J. **2007**, 53, 720-731.

(19) Sugata Pikatan Tan, Hertanto Adidharma, Maciej Radosz. Generalized Procedure for Estimating the Fractions of Nonbonded Associating Molecules and Their Derivatives in Thermodynamic Perturbation Theory. Ind. Eng. Chem. Res. **2004**, 43, 203 -208.

(20) Ziegler T. The 1994 Alcan Award Lecture: Density functional theory as a practical tool in studies of organometallic energetics and kinetics—Beating the heavy metal blues with DFT. *Can. J. Chem. Rev. Can .Chim.* **1995**, 73, 743-761.

(21) Case, D.A et al. *AMBER 8.* Univ. of California–San Francisco: San Francisco, CA, 2004.

(22) Frisch M.J.; et al. *GAUSSIAN 03,* Revision C 02. Gaussian, Inc.: Pittsburgh, PA, 2004.

(23) Charles, J. Pouchert. The Aldrich Library of FT-IR spectra (Edition I).

(24) Nakamoto, K. *Infrared and Raman Spectra of Inorganic and Coordination Compounds*, 5th Ed.; John Wiley and Sons: New York, 1997.

(25) Socrates G. *Infrared and Raman Characteristic Group Frequencies: Tables and Charts*, 3rd Ed.; Wiley: New York, 2000.

(26) Sato, T.; Shimomura, T.; Murakami, S.; Maeda, T.; Nakamura, T. Liquid-liquid extraction of divalent manganese, cobalt, copper, zinc and cadmium from aqueous chloride solutions by tricaprylmethylammonium chloride. *Hydrometallurgy* **1984**, 12, 245–254, and the references cited therein.

(27) Sato, T.; Adachi,K.; Kato, T; Nakamura,T. The extraction of divalent manganese, cobalt, copper, zinc, and cadmium from hydrochloric acid solutions by tri-n-octylamine. *Sep. Sci. Technol.* **1983**, 17, 1565-1576.

(28) Silverstein R.M.; Bassler G.C., Morrill, T.C. *Spectrometric identification of organic compounds,* 5th ed.; Wiley: New York, 1991.

(29) Gavrilko, T.; Fedorovich, R.; Dovbeshko, G.; Marchenko, A.; Naumovets, A.; Nechytaylo, V.; Puchkovska, G.; Viduta, L.; Baran J.; Ratajczak, H. FTIR spectroscopic and STM studies of vacuum deposited aluminium (III) 8-hydroxyquinoline thin films. *J. Mol. Struct.* **2004**, 704, 163-168.

(30) Mei, Q.B.; Du, N.Y.; Lu, M.G. Synthesis and characterization of high molecular weight metaloquinolate-containing polymers. *J. Appl. Polym. Sci.* **2006**, 99, 1945–1952.

(31) Yang, Q.; Jiang, J.; Chung, T.S.; Kocherginsky, N. M. Experimental and computational studies of membrane extraction of Cu (II). *A.I.CHE J.* **2006**, 52, 3266-3277.

(32) Danesi, P.R.; Horwitz, E.P.; Rickert, P.G. Rate and mechanism of facilitated americium(III) transport through a supported liquid membrane containing a bifunctional organophosphorous mobile carrier. J. Phys. Chem. 1983, 87, 4708-4715.

(33) Sillen, L. G.; Martell, A.E. *Stability constants of metal-ion complexes*, Supplement no.1; The Chemical Society: London, 1971.

(34) Sastre, A.; Madi, A.; Cortina, J.L. ; Miralles, N. Modelling of mass transfer in facilitated supported liquid membrane transport of gold(III) using phospholene derivatives as carriers. *J. Membr. Sci.* **1998**, 139, 57-65.

(35) Kocherginsky, N.M.; Yang, Q. Big Carrousel mechanism of copper removal from ammoniacal wastewater through supported liquid membrane. *Sep. Purif. Technol.* **2007,** 54, 104-116.

(36) Lamb, J.D.; Christensen, J.J.; Izatt, S.R.; Bedke, K.; Astin, M.S.; Izatt, R.M. Effect of salt concentration and anion on the rate of carrier facilitated transport of metal cations through bulk liquid membranes containing crown ethers. *J. Am. Chem. Soc.* **1980**, 102, 3399-3403.

(37) Friedman, H.L.; Krishnan, C.V. In *Water, a comprehensive treatise*, Vol.3; Plenum Press: New York, 1973, 55-58.

(38) Smith, D.W. Ionic hydration enthalpies. *J. Chem. Educ*.**1977**, 54, 540-542.

4. CHAPTER FOUR

CHARACTERIZATION AND INVESTIGATION OF AMPHOTERIC PBI NANOFILTRATION HOLLOW FIBER MEMBRANE FOR THE SEPARATION OF PHOSPHATE, BORON, ARSENATE AND COPPER IONS

4.1 Introduction

Toxic species, such as phosphate, arsenate, borate and copper ions are known to have adverse effects on human health and a higher than allowed level of these toxic species in surface and ground waters has become a major health problem in many countries all around the world. The presence of phosphate in the effluent discharged to natural bodies has long been known to be responsible for the eutrophication [1]. Phosphate removal can be achieved by adsorption, precipitation and electrocoagulation [1-4]. Boron is a typical drinking water contaminant affecting the reproductability of living organisms. Boron and arsenic can be removed by adsorption, ion exchange, electrocoagulation method and precipitation etc [5-8]. For the adsorption process, activated alumina and ion exchange resin have been demonstrated to be effective in removing arsenic from water. Arsenate sorption occurs best at pH 6.0 ~ 8.0 where activated alumina surfaces are positively charged. Arsenite adsorption is strongly pH dependent and it exhibits a high affinity towards activated alumina at pH 7.6 [9]. Studies have shown that the ion exchange resin strongly adsorbed arsenite from pH 5 to 10 and arsenate from pH 1 to 5 [10]. For the precipitation process, four precipitation processes: alum coagulation, iron coagulation,

lime softening, and a combination of iron (and manganese) are useful for arsenic removal [11]. Concerns on the existence of heavy metal ions, e.g. copper ions, in the aquatic environment have also been a subject of importance due to their toxicity. A lot of treatment methods have been employed to remove heavy metal ions from the waste, such as extraction, sorption and ion exchange [12-15]. Several different sorbents such as natural clays, biopolymeric sorbent vermiculite and activated carbon have been investigated in terms of decontamination of the discharged effluents and concentration of heavy metal ions [16-19]. Ion exchange processes have also been demonstrated to remove heavy metal ions including copper from the wastewater effectively [20-21].

However, the limitations of these technologies for these toxic species removal should be further considered. For example, the solvent extraction process suffers from drawbacks, such as a large amount of solvent consumption, solvent degradation and inadequate decontamination efficiency [22]. The adsorption methods are confronted with some problems, such as poor selectivity and slow regeneration. For ion exchange processes, it is difficult to develop novel ion exchange resins with highly selective functional groups for greater selectivity for the removal of contaminants alone.

Membrane separation processes have been determined to be a feasible option for removal of toxic species, such as phosphate, arsenate, arsenite, borate and copper ions. Reverse osmosis (RO) membranes have been tested for the treatment of wastewater to reduce fresh water consumption and environmental degradation [23-25]. However, reverse osmosis (RO) still suffers from limitations such as the fouling of membranes,

consumption of a large amount of water, slow treatment, high operating pressures and low selectivity for the fractionation of monovalent ions. In order to overcome these issues, the use of low-pressure membrane processes has been investigated. For instance, the membrane distillation through porous membranes [26], the applications of liquid membranes [27-29] have been studied, but they also have many drawbacks in terms of toxic species removal efficiency, the volume of water consumption and process stability. Nanofiltration (NF) of wastewater for toxic species removal has also been carried out [30]. However, there has been little study reported on separation of many toxic species by using one only kind of NF membrane which not only useful for cations removal but also anions removal.

Over the last 15 years, NF as a relatively new pressure-driven membrane process has received a lot of attention because NF has a widening range of application for liquid-phase separations, such as in water treatment, pharmaceutical and biotechnology. Nanofiltration membranes perform separation in between those of porous ultrafiltration (UF) membranes and non-porous reverse-osmosis (RO) ones. NF has two interesting features: one is that the MWCOs (molecular weight of the solute that is 90% rejected by the membrane) range from 200 to 1000 due to the pore diameters ranging from 0.5 nm to 2 nm; another one is that most of NF membranes are either positively-charged or negatively-charged [31]. Therefore, the NF separation mechanisms involve both steric-hindrance and electrostatic (Donnan) effects. For the separation of uncharged solutes, size effect is the governing factor to determine the solute permeation. However, the NF processes to separate the charged ions are mainly determined by the electrostatic

interaction between the solute species and the charged NF membranes. Hence, for the transport of charged solutes, the membrane charge characteristics play a significant role. Consequently, the investigation of the membrane charge properties is of great importance. There are a lot of investigations have been done to evaluate the separation performance of cations, e.g. copper, and anions, e.g. borate ion, phosphate, arsenate or arsenite using respective NF membranes [32-35]. Generally, positively-charged NF membranes are only effective for cations removal, whereas negatively-charged NF membranes are only effective for anions removal. There is few amphoteric nanofiltration membranes reported which could exhibit different charges at different pH ranges, subsequently show efficient separation performance on both cations and anions based on the solution pH. The purpose of this work is to investigate the charge characteristics of the amphoteric polybenzimidazole (PBI) NF membranes and explore the potential of PBI NF membranes using as candidate membrane for the removal of both cations and anions which are environmentally concerned. The chemical structure of PBI is shown in Fig.4.1. Moreover, the PBI NF membrane in hollow fiber configuration is fabricated because of its many advantages over flat sheet membranes [36].

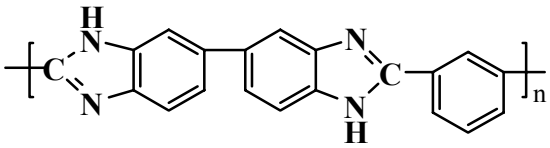

Fig. 4.1. Chemical Structure of polybenzimidazole (PBI)

In this particular study, the primary research interests are located in the membrane charge characteristics determination based on the rejection of NaCl under different pH. Because the separation performance of different valent cations and anions is another important characteristic, nanofiltration of different types of salts is also performed, including types of 1-1 (NaCl), 1-2(Na_2SO_4), 2-1 ($MgCl_2$) and 2-2 ($MgSO_4$). Typical toxic anions of phosphate, borate ion, arsenite and arsenate and typical toxic cations of copper which have suspected teratogenetic properties and are suspect carcinogens [32-35, 37] are major concern in the water treatment and therefore separation performance of these toxic ions is also investigated. The effects of chemical nature of solutes, concentration of salts and the feed pH on the separation performance of the PBI membrane are systematically investigated.

4.2. Experimental section

4.2.1 Materials

Various charged solutes were employed to study the transport properties and separation performance of the PBI NF membrane. They are NaCl, $MgCl_2$, $MgSO_4$, Na_2SO_4, $CuSO_4{\cdot}5H_2O$, $CuCl_2$, H_3BO_3, Na_3PO_4, Na_2HPO_4, NaH_2PO_4 and $NaH_2AsO_4{\cdot}7H_2O$ purchased from Aldrich Sigma, Singapore. Properties of these ions are listed in Table 4.1 [38-42]. NaOH (1.0N), KOH (1.0N) and HCl (1.0N) solutions were used to adjust the pH of feed solutions. All chemicals were used as received. Ultrapure water used in all

experiments was produced by a Milli-Q unit (MilliPore, USA) with a resistivity of 18.2 MΩ cm.

Table 4.1. Ion and electrolyte diffusivities and hydrated radii (at 25ºC)

Ions	Ion diffusivities (10^{-9} m^2/s)	Hydrated Radius (nm)	MW (g/mol)
H^+	9.31	0.28	1.0
Na^+	1.33	0.36	23.0
Mg^{2+}	0.72	0.43	24.0
Cu^{2+}	0.72	0.42	63.5
Cl^-	2.03	0.33	35.5
SO_4^{2-}	1.06	0.38	96.0
$H_2PO_4^-$	0.47	0.30	98.0
HPO_4^{2-}	0.44	0.33	97.0
PO_4^{3-}	0.43	0.34	96.0
$HAsO_4^{2-}$	0.32	----	139.9
H_3AsO_3	1.03	----	125.9

Table 4. 2. Pure water permeability (PWP), the effective pore radius (r_p), geometric standard deviation (σ_p) , molecular weight cut off (MWCO) and ratio of membrane porosity over thickness ($A_k/\Delta x$) of PBI hollow-fiber membrane

Pure water permeability PWP, ($l\ m^{-2}\ bar^{-1}\ h^{-1}$)	r_p (nm)	σ_p	MWCO (Da)	$A_k/\Delta x$ [$10^6\ m^{-1}$]
1.86	0.348	1.53	525	0.128

4.2.2 PBI nanofiltration hollow fiber membrane

The PBI nanofiltration hollow fiber membrane studied in this work was fabricated through the phase inversion process described elsewhere [43]. Fig. 4.2 illustrates its structure which consists of four types of morphologies: asymmetric outer-selective skin, an array of very small yet elongated fingerlike macrovoids near the outer layer, a spongy-like substructure near the inner skin and porous inner skin. This kind of microstructure can withstand high transmembrane pressures. Table 4.2 summarizes its pure water permeability (PWP), the effective pore radius (r_p), geometric standard deviation (σ_p) and molecular weight cut off (MWCO), while Fig. 4.3 shows its pore size distribution from the solute transport method [44]. A bundle of PBI hollow fibers were loaded in a stainless tube (20 cm in length) and sealed with epoxy at two ends to form a membrane module with the effective area of about 100 cm^2, which was used to test the separation performance and the ion transport property.

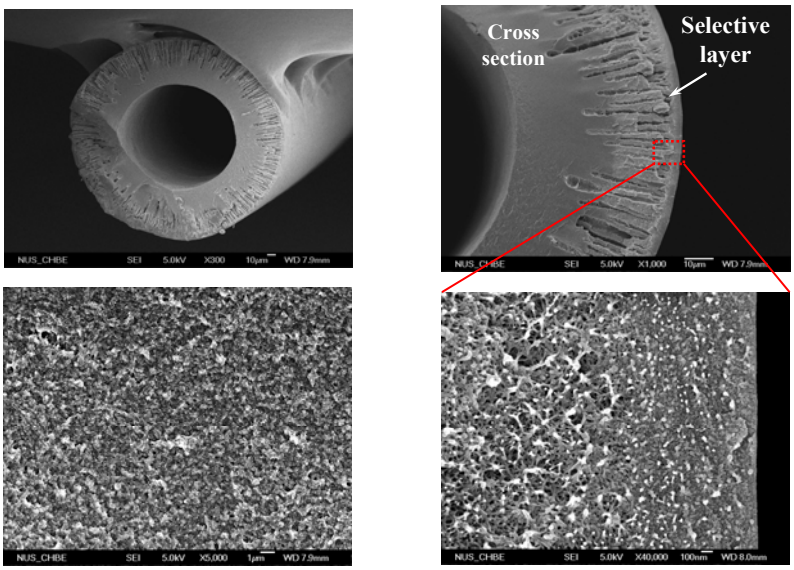

Fig 4.2. Morphology of asymmetric PBI nanofiltration hollow fiber membrane.

4.2.3 Nanofiltration experiments with PBI nanofiltration hollow fiber membranes

The following describes the experimental designs and separation procedures:

(1) Neutral solutes were dissolved in ultrapure water with concentrations of about 200 ppm to form feed solutions. These feed solutions were circulated in the NF systems for about 0.5 h to ensure the systems reach the steady state. During the experiments, the temperatures of feed solutions were maintained at 20±0.1°C by employing a heat exchanger inside the feed tank. The NF experiments were carried out from lower molecular weights to higher molecular weights. The PBI NF membranes were thoroughly flushed by pure water between nanofiltration of different solutes with different molecular

weights. These rejections of different solutes and the molecular size of these neutral solutes were used to calculate NF membrane's pore size distribution and mean pore size.

(2) NaCl solutions at a concentration of 3.4 mM with different pH values were prepared. The rejections of these NaCl solutions by PBI NF membranes were tested under different pressures.

(3) NaCl solutions with different concentrations (1mM, 3.4mM, 10mM and 100mM) were prepared. The rejections of these different concentrations of NaCl solutions by PBI NF membranes were tested under different pressures.

(4) Copper chloride, copper sulphate, phosphate solutions, boron acid solution, As(V) were prepared by dissolving $CuSO_4 \cdot 5H_2O$, $CuCl_2$, Na_3PO_4, Na_2HPO_4, NaH_2PO_4, boric acid and $NaH_2AsO_4 \cdot 7H_2O$ in ultrapure water, respectively. Unless otherwise stated, concentrations of all salts were 1mM and those of As(V) were at 0.1mM. The solution pH was modified by additions of KOH (1.0N) and HCl (1.0N) solutions. The NF of these slats was conducted as described in the step (1) with testing sequences from pH 5.5 to 13.0 and finally pH 3.1.

Concentrations of the neutral solute solutions were measured with a total organic carbon analyzer (TOCASI-5000A, Shimazu, Japan). The concentrations of choloride in the aqueous phase were analyzed by using an ion chromatograph (Metrohm Model 702) equipped with a conductivity detector and a Hamilton PRP-X 100 anion column was used.

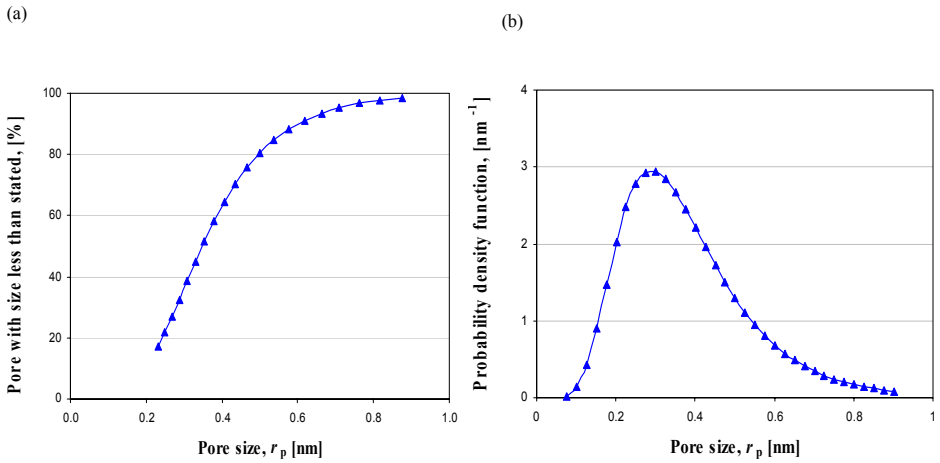

Fig. 4.3. (a) Cumulative pore size distribution curves;
(b) Pore size probability density function curves of the PBI hollow fiber membranes

It was operated at a flow rate of 2 ml/min with an eluent containing 1.7 mM $NaHCO_3$ and 1.8 mM Na_2CO_3. The solution pH was measured by a pH meter (Orion PerpHect pH meter 370, USA). Concentrations of Cu(II), arsenic, boron and phosphorus were detected by a Perkin Elmer Optima 3000 ICP-AES (Norwalk, CT). Generally, the observed rejections during the NF are defined as follows:

$$R_{obs} = 1 - \frac{C_p}{C_b} \tag{4.1}$$

where C_p and C_b are solute concentrations in the permeate and bulk feed side, respectively. The true or real rejection at the membrane surface, R_T, is defined as:

$$R_T = 1 - \frac{C_p}{C_m} \tag{4.2}$$

where C_m is the solute concentrations on the membrane surface. The real rejection of R_T was obtained following the procedure described elsewhere [45].

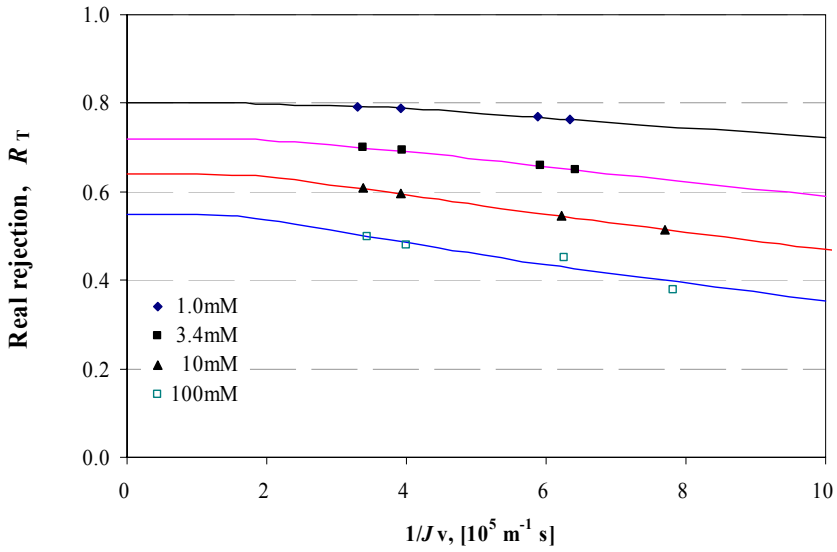

Fig. 4.4. Real rejection as a function of permeate volume flux J_V with different NaCl concentrations. The curves are fitted by the Spiegler–Kedem equations 4.4-4.5.

4.3 Results and Discussion

4.3.1 Characterization of PBI membranes using NaCl solutions

In order to investigate the charge and separation characteristics of PBI membranes, the nano-transport and separation of NaCl at different pressures and different concentrations

from 1 to 100 mol m^{-3} were conducted. As shown in Fig. 4.4, an increase in NaCl feed concentration results in a decrease in NaCl rejection. This is due to the anion shielding effect on the effective membrane charge density.

Solute transport phenomena of the nanofiltration process can be described by irreversible thermodynamics. Kedem and Katchalsky [46] proposed the relation of the volumetric flux J_v and the solute flux J_s through a membrane based on the following equations:

$$\begin{aligned} J_v &= L_P(\Delta P - \sigma\Delta\pi), \\ J_s &= P(C_f - C_P) + (1-\sigma)J_v\bar{c} \end{aligned} \tag{4.3}$$

Eq. 4.3 indicates that transport across a membrane is characterized by three transport parameters, i.e. the pure water permeability L_p, the reflection coefficient σ, the solute permeability P. When concentration difference between the feed side and the permeate is high, Spiegler and Kedem [47] improved this model to express in a differential form as follows:

$$J_s = -P'(\frac{dc}{dx}) + (1-\sigma)J_v c \tag{4.4}$$

where P' is the local solute permeability defined as $P' = P\Delta x$. Integrating Eq. 4.4 across the membrane thickness yields the Spiegler–Kedem equation:

$$R_T = 1 - \frac{c_P}{c_m} = \frac{\sigma(1-F)}{1-\sigma F}, where F = \exp(-((1-\sigma)/P)J_v) \tag{4.5}$$

The Spiegler–Kedem equation usually applied when there is no electrostatic interaction between the membrane and the neutral solutes. From Eq. 4.5, one can see that the reflection coefficient σ corresponds to the maximum rejection at an infinitely high permeate volume flux. The values of σ and P can be determined directly from

experimental data of the real rejection R_T, as a function of J_v by any best-fitting method. Fig. 4.5 shows their values plotted against NaCl concentrations.

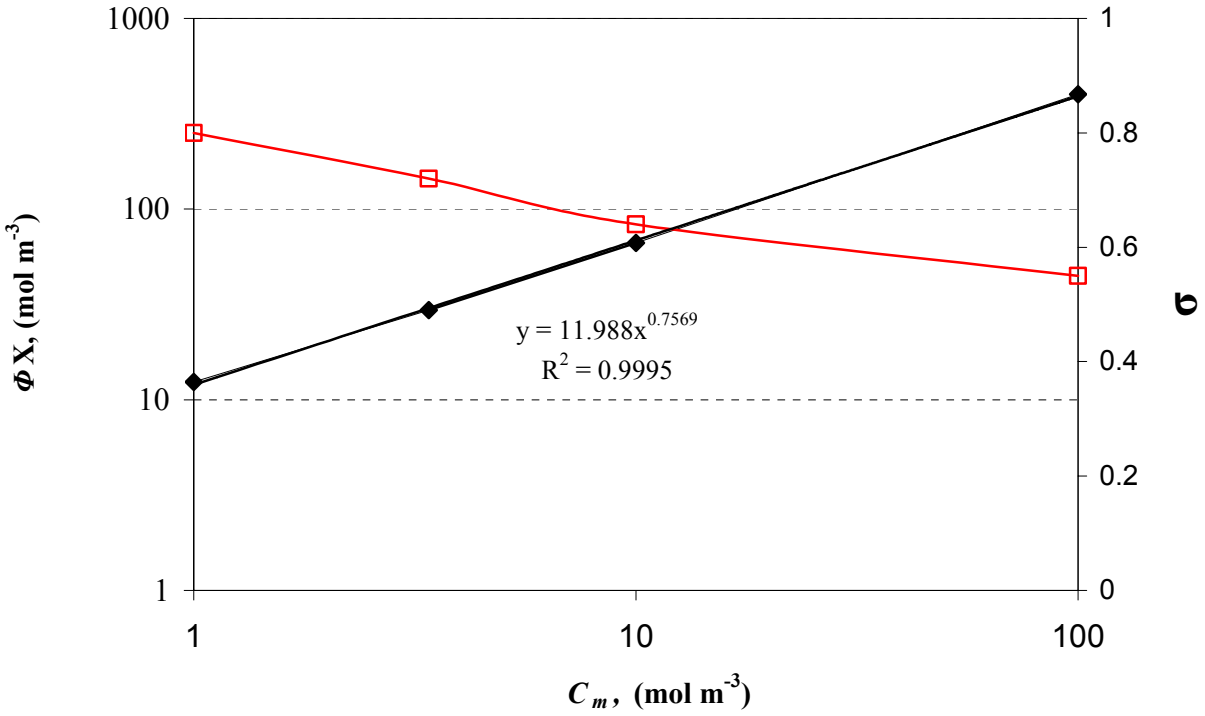

Fig. 4.5. Reflection coefficient and effective charge density of PBI membrane as a function of NaCl concentration.

For a system of a 1-1 type electrolyte and NF, by combining the extended Nernst–Planck equation and the Donnan equilibrium theory, membrane parameters σ and P can be determined based on the Teorell-Meyer-Sievers (TMS) model with the following equations [48]:

$$\sigma = 1 - \frac{2}{(2\alpha - 1)\xi + (\xi^2 + 4)^{0.5}}$$
$$P = D_s(1-\sigma)\left(\frac{A_k}{\Delta x}\right) \quad (4.6)$$

where ξ is defined as the ratio of effective volume charge density (X) of membrane to the electrolyte concentration (C_m) at the membrane surface, α is the transport number of

cations in free solution defined as $\alpha = D_1/(D_1+D_2)$. D_1, $D_2 = 1.33\times10^{-9}$, 2.03×10^{-9} m^2 s^{-1}, respectively, based on Table 4.1. Therefore, the effective charge density of PBI NF membrane can be determined as a function of NaCl concentration if σ and α are available, as shown in Fig. 4.5. At a higher NaCl concentration, the membrane seems to have a larger calculated charge density. The effective charge density ϕX can be related to NaCl concentration by the following empirical Eq. (4.7) as shown in Fig. 4.5 [48, 49]:

$$\phi X = KC_m^{\ n} \tag{4.7}$$

The dependency of separation performance of the PBI NF membrane on surface charge, which is influenced by the pH of the contacted aqueous solutions, has been carried out.

As shown in Fig. 4.6, a V-shape trend of NaCl rejection by the PBI membrane reflects the surface charge characteristics under different pH values, which are quite similar to the behavior of amphoteric ceramic membranes (which have the metal oxide group) [50, 51]. A minimum ion rejection appears at pH 7.0 (close to the pK_a of the imidazole group within PBI molecules). This implies that the PBI membrane has an isoelectric point near pH 7.0 and has different charge signs based on pH of the media, i.e. may be positively charged at low pH and negatively charged at high pH. This phenomenon could be attributed to the unique amphoteric structure of imidazole group within PBI molecules.

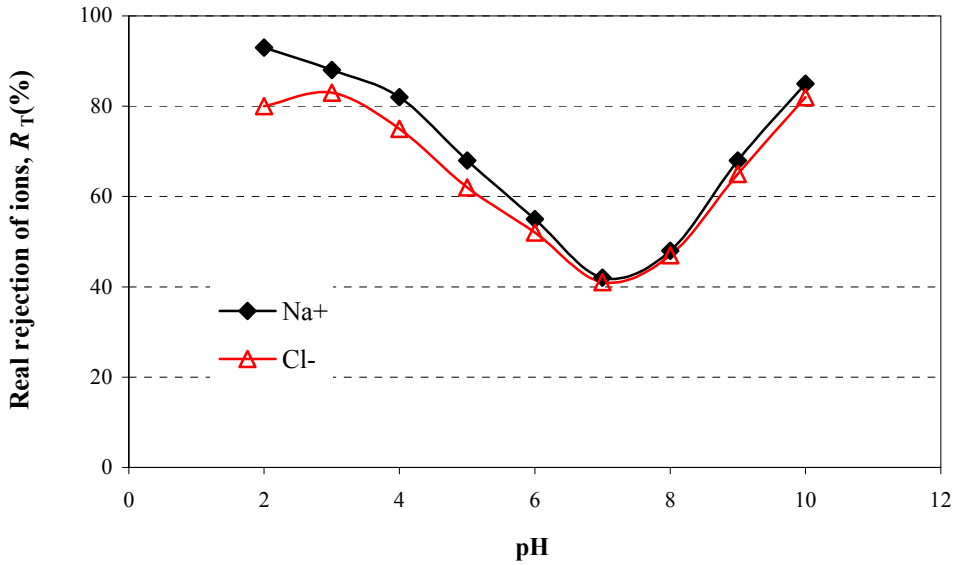

Fig. 4.6. Rejection of NaCl (1.0 mol m^{-3}, 20ºC) as a function of pH
(Adjusting the solution pH through adding 1.0 N HCl or 1.0 N NaOH solutions)

4.3.2 Transport of various single electrolytes through the PBI membrane

Fig. 4.7 compares the separation characteristics of four types of single salts, i.e. NaCl, $MgCl_2$, Na_2SO_4 and $MgSO_4$, at the same molar concentration (1.0 mol m^{-3}) and pH 7.0 under different pressures and demonstrates that the PBI NF membrane exhibits different rejections to various valent anions and cations. The salt rejections follow the order of $R_T(MgCl_2) > R_T(MgSO_4) > R_T(Na_2SO_4) > R_T(NaCl)$. Investigation shows that the PBI NF membranes demonstrate the highest rejection to divalent cations, a lower rejection to divalent anions and the lowest rejection to monovalent ions. The hydrated radii of ions as

listed in Table 4.1 are partially attributed to this rejection trend. In addition, the solute

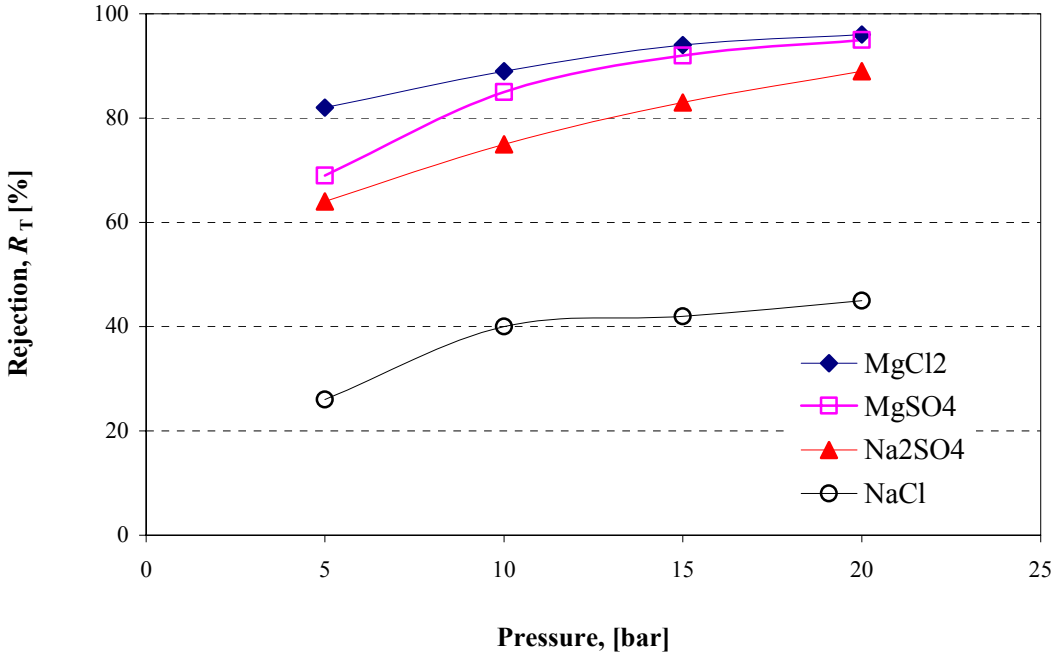

Fig. 4.7. Rejection of different salts as a function of pressure
(Bulk solution concentration of single salt solutions: 1.0 mol m^{-3}, pH 7.0).

rejection increases with applied pressures. This observation can be explained by the fact that the water flux is linearly related to the applied pressure, whereas the solute flux is dependent on several factors: the concentration gradient over the membrane; the interaction between solute and water; and the water permeate flux. Therefore, the water permeate flux increases relatively faster than the solute flux with an increase in the applied pressure, resulting in a decrease in solute permeates' concentration and therefore an increase in solute rejection.

4.3.3 Separation of phosphate

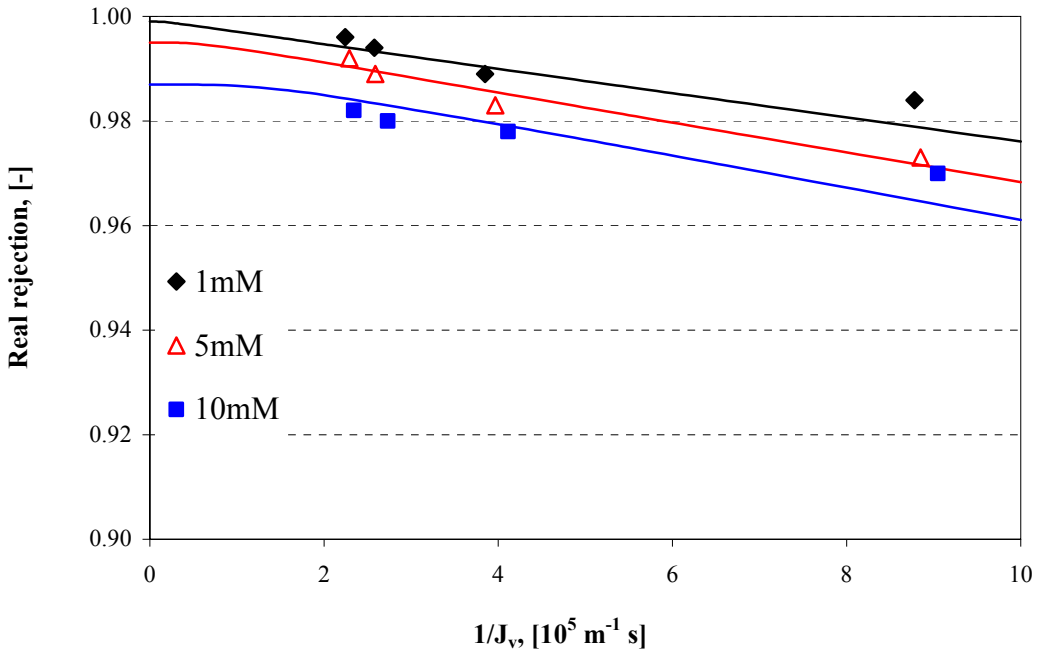

Fig. 4.8. Real rejection as a function of permeate volume flux J_V with different Na_3PO_4 concentrations. The curves are fitted by the Spiegler–Kedem equations 4.4-4.5.

Table 4.3 σ and P of various concentrations of Na_3PO_4 determined from the Spiegler–Kedem equations.

Na_3PO_4	Reflection coefficient σ	Permeability [10^{-8} m·s^{-1}]
1 mM	0.999	2.4
5 mM	0.995	3.0
10 mM	0.987	3.3

Fig. 4.8 shows the Na_3PO_4 rejection vs. reciprocal of permeate volume flux with various concentrations. The rejection of phosphate decreases with increasing concentration, which can be explained by the cation shielding effect on the membrane charge density. Solid lines in Fig. 4.8 were derived from the nonlinear least-squares regression analysis based on the Spiegler-Kedem equations. Table 4.3 summarizes the calculated σ and P, and shows that the lower the Na_3PO_4 concentration, the higher the reflection coefficient and the lower the solute permeability.

Table 4.4 σ and P of Na_3PO_4, Na_2HPO_4 and NaH_2PO_4 at a concentration of 1mol m^{-3} determined from the Spiegler–Kedem equations.

	Reflection coefficient σ	Solute permeability P [10^{-8} m·s^{-1}]
Na_3PO_4	0.999	2.40
Na_2HPO_4	0.985	8.05
NaH_2PO_4	0.87	26.0

Fig. 4.9 shows the phosphate rejection in the sequence of $R_T(PO_4^{3-}) > R_T(HPO_4^{2-}) > R_T(H_2PO_4^{-})$ at a concentration of 1.0 mol m^{-3}. Table 4.4 tabulates the calculated σ and P of Na_3PO_4, NaH_2PO_4 and $NaHPO_4$ by curves fitting with the aid of the Spiegler–Kedem equations. The reflection coefficient, σ, follows the trend of σ $(PO_4^{3-}) > \sigma$ $(HPO_4^{2-}) > \sigma$ $(H_2PO_4^{-})$, whereas the permeability P exhibit the trend of P $(PO_4^{3-}) < P$ $(HPO_4^{2-}) < P$

($H_2PO_4^-$). These sequences can be attributed to two factors: namely, the Donnan exclusion and size effects. The former suggests that enhanced charge exclusion occurs between the multivalent anion and the membrane, while the latter indicates a greater rejection for large size ions. The hydrated radii of these ions are as follows: $r_h(H_2PO_4^-)$ = 0.30 nm, $r_h(HPO_4^{2-})$ = 0.33 nm, and $r_h(PO_4^{3-})$ = 0.34 nm [40].

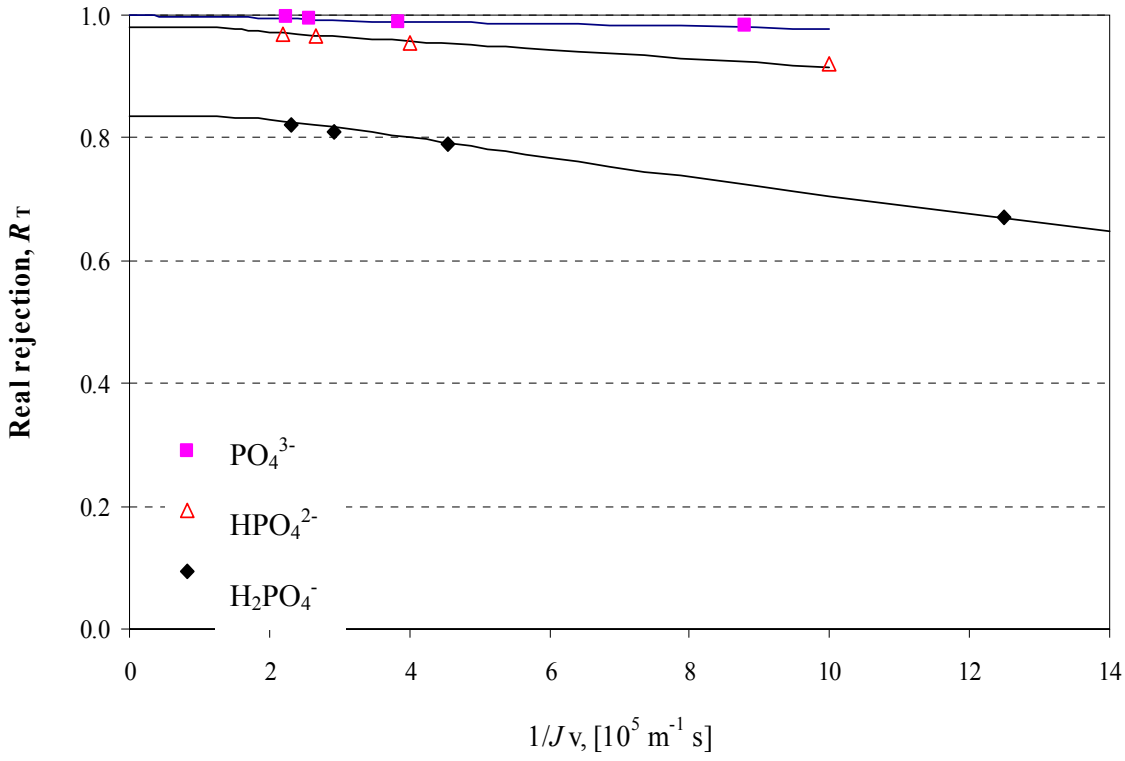

Fig. 4.9. Real rejection as a function of permeate volume flux J_V with different phosphate at a concentration of 1.0 mol m^{-3}. The curves are fitted by the Spiegler–Kedem equations.

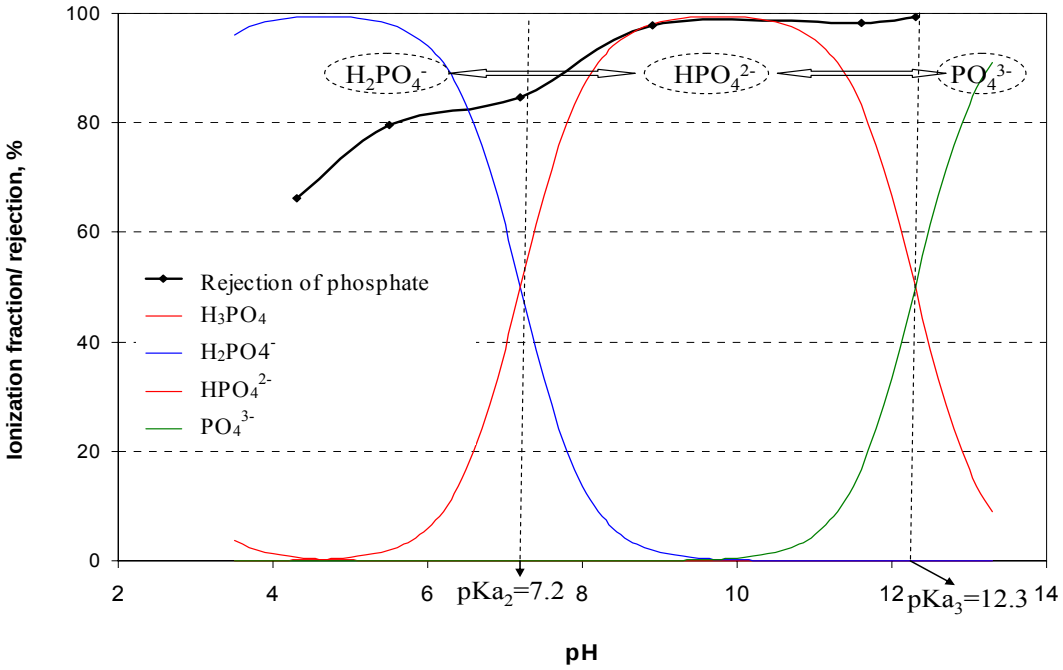

Fig. 4.10. Speciation of phosphate and rejection by PBI membrane as a function of feed solution pH (feed concentration =1 mol m^{-3})

In addition, the feed pH influences the membrane properties, e.g. surface charge signs, surface charge density, hydrophilicity and porosity because pH determines the major phosphate species based on the phosphate-H_2O equilibrium as shown in Fig 4.10. As is clearly showed, H_3PO_4 species is predominant in the range of pH 3.0-4.7. Around pH 7.2, monovalent anions of $H_2PO_4^-$ and divalent HPO_4^{2-} co-exist and their fractions are dependent on the solution pH. In the range of pH 7.2-11.0, the major phosphate species present becomes divalent anions of HPO_4^{2-} and the membrane may be negatively charged, which consequently results in an increase in the rejection of phosphate. As the pH>12.3, the major phosphate species becomes trivalent PO_4^{3-}. From the rejection curve, the phosphate rejection increase from 66.2% to 84.7% when the pH of solution increases from 4.3 to 7.2. This observation can be attributed to the combination of the increase of HPO_4^{2-} percentage and the membrane becoming increasingly negative. From pH 7.2 to 12.3, the phosphate rejection rises from 84.7% to 99.4%. Similarly, this is due to the fact

that the PO_4^{3-} percentage increases and the negatively-charged PBI membrane. Thus, the solution pH has the dominant effect on the phosphate rejection because pH determines the ionization fraction of phosphate, their sizes, and the surface charge characteristics of the PBI membranes.

4.3.4 Separation of arsenate As(V)

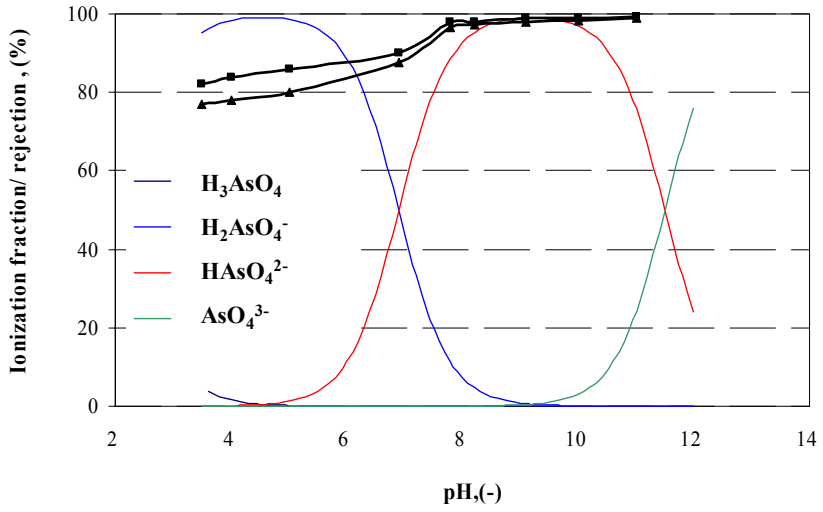

Fig. 4.11 Speciation of arsenate As(V) and rejection by PBI membranes as a function of feed solution pH (feed concentration = 1 mol m^{-3})

The increase in As (V) rejection with pH can be attributed to two reasons. Firstly, as can be seen from the ionization fraction curve of As(V), the speciation of As(V) changes from monovalent ($H_2AsO_4^-$, $pK_{a2} \sim 6.9$) to divalent ($HAsO_4^{2-}$). The rejection of $H_2AsO_4^-$ is much lower than divalent species due to the enhanced electrostatic interaction between divalent ions with the membrane. Secondly, as pH increases above 7.0, the PBI membrane charge becomes negative, which is the same charge sign with the anions.

Therefore, the charge exclusion becomes more significant at pH > 7.0 and so does the rejection.

$$H_3AsO_4 \rightleftharpoons H_2AsO_4^- + H^+ \rightleftharpoons HAsO_4^{-2} + 2H^+ \rightleftharpoons HAsO_4^{-3} + 3H^+, \text{ p}K\text{a } 2.2, 6.9, 11.5 \qquad (4.8)$$

The rejection of As (V) as a function of pH values also measured in the presence of 10mol m^{-3} NaCl. The rejection has been promoted when the NaCl is present; this is most likely attributed to the presence of the more mobile Cl^- co-ions as shows in the Table 4.1. Therefore, it is expected that the As(V) removal could increase in the presence of the more permeable ion.

4.3.5 Boron separation by PBI NF membranes

Boron separation experiments were carried out under different pH values from 4 to 11 adjusted by 1N NaOH or 1N HCl. However, the boron acid concentration was fixed at 1.0 mol m^{-3}. Generally, boron exists in natural water in the form of boric acid, and the dissociation of boric acid is dependent on the solution pH as illustrated below. The pKa value of B(III)-H_2O equilibrium equals to 9.1 [52].

$$B(OH)_3 + H_2O \rightleftharpoons B(OH)_4^- + H^+, \text{ p}K\text{a } 9.1 \qquad (4.9)$$

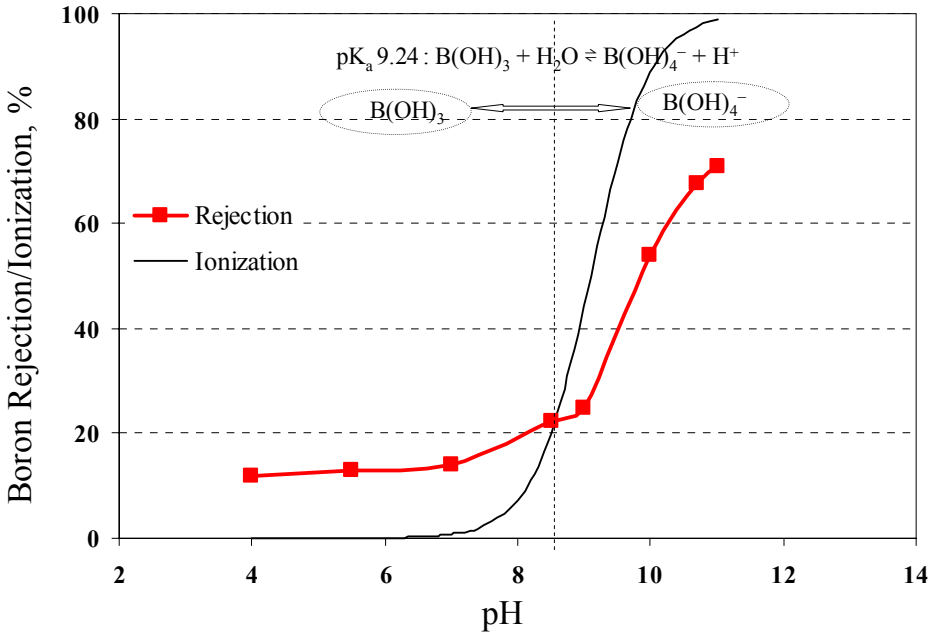

Fig. 4.12. Ionization of boric acid and rejection by PBI membranes as a function of solution pH (feed concentration = 1 mol m^{-3})

Fig. 4.12 shows that boric acid can be efficiently rejected only in the dissociated ionic form which occurs at a relatively high pH (i.e., >10). The rejection of boron increases from 25% to 70% when the feed pH increases from 9.0 to 11.0. Similar to the previous As(V) case, the increase in rejection can be attributed to three reasons. As can be seen from the ionization fraction curve of boron acid, the speciation of boron acid changes from uncharged $B(OH)_3$ to monovalent anion $B(OH)_4^-$. Since the rejection of the uncharged species is much lower than monovalent species, the former has a less rejection than the latter. In addition, based on the Cerius2 molecular simulation as shown in Fig. 4.13, the monovalent anion $B(OH)_4^-$ is more like a sphere with the diameter of 6.8 Å, whereas the uncharged $B(OH)_3$ molecule is flat and more like a plate with 4.6 Å in length and 1.4 Å in thickness. Therefore, by taking the molecular configuration into account, the steric hindrance for a monovalent $B(OH)_4^-$ anion should be much greater than that of an uncharged $B(OH)_3$ molecule. Furthermore, as the pH value increases, the PBI membrane

becomes more negative charged, and therefore the repulsion between $B(OH)_4^-$ and membrane increases, which resulting in an enhancement in boron rejection. This phenomenon has also been observed by other investigators [53, 54]. Because the highest boron rejection is still less than 80%, it can be concluded that boron cannot be simply removed by one-stage nanofiltration. Therefore, a combination with adsorption and/or ion-exchange to partially remove the boron and then followed by a multiple stage of NF systems operated at pH values of 10-11 is necessary for the effective removal of boron before discharging into the environment.

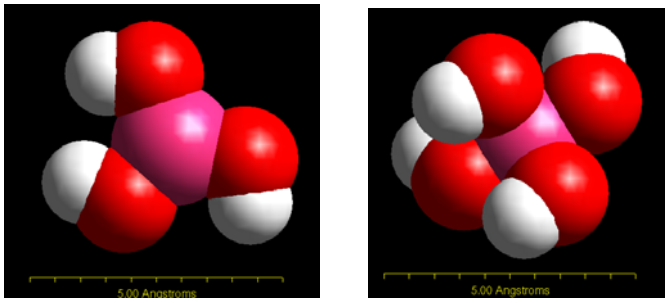

H_3BO_3 $B(OH)_4^-$

Fig. 4.13. Molecular configurations simulated from Cerius 2

4.3.6 Separation of copper sulfate and copper chloride

Because the free copper Cu(II) cations could precipitate out from neutral or alkaline solutions, rejection of copper cations by the PBI membrane is conducted in acidic solutions of various pH levels with the presence of $CuSO_4$ or $CuCl_2$ as depicted in Fig.

4.14. For both $CuSO_4$ and $CuCl_2$ solutions, the rejection of Cu(II) cation is found to be increased with increasing solution pH level. This is due to the fact that the PBI membrane is positively charged at pH < 7.0, but the positive charge decreases with increasing pH value, resulting in the low permeate of the anions; therefore in order to maintain the electroneutrality of the permeate solution, rejection of the Cu^{2+} increases.

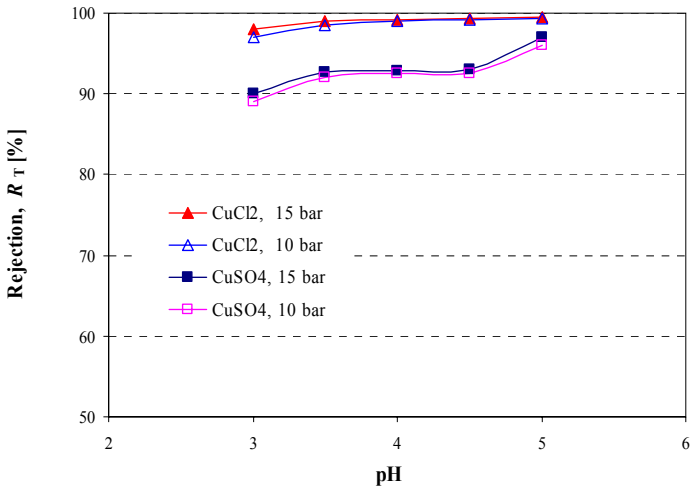

Fig. 4.14. Rejection of Cu (II) vs. solution pH under different pressures.
Salt concentration, 1.0 mol m^{-3}

In addition, the rejection of $CuCl_2$ is much higher than that of $CuSO_4$ due to effect of counter anions although SO_4^{2-} has a bigger size than Cl^-. For the stronger ionic charge density of SO_4^{2-} than that of Cl^-, the rejection of Cu^{2+} by the positively charged PBI membrane would be weakened accordingly. That is to say, the decreased rejection with the multi-valent anions is attributed to the stronger attraction between the negative charged SO_4^{2-} and the positively charged PBI membrane.

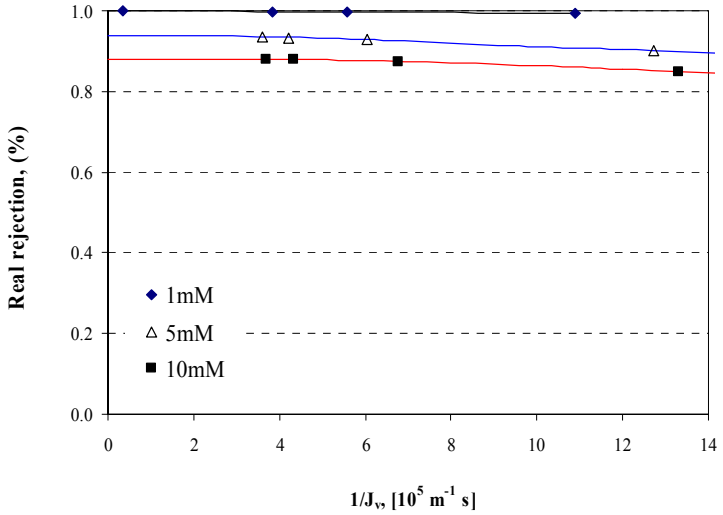

Fig. 4.15. Real rejection as a function of permeate volume flux J_v with the different $CuCl_2$ concentrations. The curves are fitted by the Spiegler–Kedem equations. pH 5.0

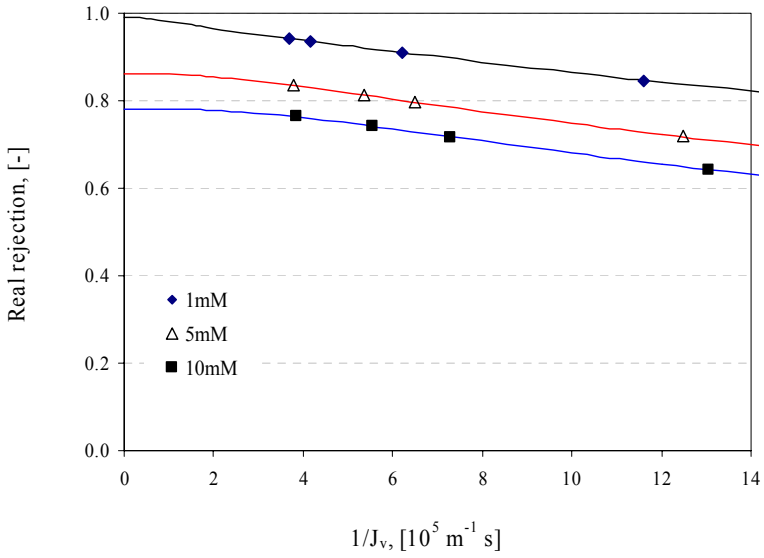

Fig. 4.16. Real rejection as a function of permeate volume flux J_v with the different $CuSO_4$ concentrations. The curves are fitted by the Spiegler–Kedem equations.

Fig. 4.15 and 4.16 show the rejections of $CuCl_2$ and $CuSO_4$, respectively, as a function of permeate flux with various concentrations at about pH 5. The membrane parameters are fitted based on the Spiegler-Kedem equation. The rejection of PBI hollow-fiber

membrane to $CuCl_2$ and $CuSO_4$ increase with the growth of the permeate flux. Actually, this is a generally true because the increase of the applied pressure results in a higher water flux whereas the cation and anion are sterically and electrically hindered. Rejections of Cu^{2+} cation in $CuCl_2$ and $CuSO_4$ solutions decrease with increasing feed concentration. The reason is that increasing the chloride and sulfate concentration involves the formation of a screen which gradually neutralizes the charge of the membrane. The decrease in the effective charge of the PBI membrane leads to the decreased Cu^{2+} rejection since the electrostatic effects of the membrane become weaker. This result can be linked to the dependence of the effective charge density of the membrane on the electrolyte concentrations.

Table 4.5 σ and P of various concentrations of $CuCl_2$ and $CuSO_4$ determined from the Spiegler–Kedem equations.

Concentration	**σ**	**P [10^{-7} m·s^{-1}]**
(mol m^{-3})	**$CuCl_2$**	
1	0.999	0.044
5	0.937	0.53
10	0.880	0.62
(mol m^{-3})	**$CuSO_4$**	
1	0.991	1.52
5	0.862	2.14
10	0.782	2.41

Table 4.5 summarizes the calculated σ and P as a function of $CuCl_2$ and $CuSO_4$ concentration with the aid of the data fitting method using the Spiegler-Kedem equation. The reflection coefficient of $CuCl_2$ by the PBI membrane is higher than that of $CuSO_4$ at

each concentration. This result is consistent with Figure 4.14, indicating that the NF PBI membrane exhibits a higher degree of membrane perfection (i.e., higher reflection coefficient) in the $CuCl_2$ solution than in the $CuSO_4$ solution. In other words, the degree of membrane perfection apparently play a comparable role as membrane charge characteristics when comparing the rejection of $CuCl_2$ and $CuSO_4$ via the PBI NF membrane. Table 4.5 also shows that the Cu^{2+} permeability increases with an increase in solution concentration. This phenomenon may arise from the fact that the effective area of the membrane pore becomes larger due to decreased thickness of electrical double layer (EDL) [55]. Similar observations have been reported in the literature in NF membrane separation data [56, 57].

4.3.7 Comparison with other NF membranes

Van Voorthuizen et al [58] employed commercial membranes NF 90 and NF 200 to separate Na_2HPO_4 at a concentration of 1mol m^{-3} with rejections of 98% and 97%, respectively. Visvanathan and Roy [59] demonstrated that Desal-5 NF membranes rejected phosphate at a rejection of 95%-99%. The investigated PBI membranes exhibit a comparable rejection, 98.2%, with these commercial NF membranes at the same concentration indicating that the PBI membrane is a good candidate for phosphate removal. Sato et al [60] investigated three kinds of NF membranes, ES-10, NTR-729HF and NTR-7250 for arsenate removal at pH 6.8 with rejections of 85%-86%, 91%-94%, 95-97%, respectively. And their rejections for arsenite removal are 10-15%, 15%-25%, 60%-80%. At pH 6.8, the rejections of arsenate and arsenite by PBI NF membranes in

this work are 87.7% and 33%, respectively. The rejections of both arsenate and arsenite are comparable with or even better than those of commercial membranes. Dydo et al [61] employed three NF membranes, BW-30, TW-30 and NF-90, to separate borate ions under 41atm at various pH in the range from 8.0 to 11.0. At pH of 11.0, the boron rejections for BW-30, TW-30 and NF-90 membranes are 98.4%, 97.6% and 97.2%, respectively. Whereas the boron rejection for the PBI NF membrane is 71% at pH of 11.0 under the operating pressure of 15 bar in this work. It is expectable that the boron rejection for the PBI NF membrane will increase with the applied pressure to a value which is comparable with that of the above-mentioned commercial membranes. Investigation of the performance of Desal polyamide composite membrane on copper removal has been carried out [62]. The copper rejection of $CuSO_4$ and $CuCl_2$ for the Desal polyamide composite membrane at a constant pressure (Δp=100psi) and at pH 4.5 is 98.1% and 93.1%, respectively. Nanomax 50 has also been investigated for copper removal at a pressure of 10 bar and at pH 4.5 with copper rejections of 98.4% and 82.8% for $CuSO_4$ and $CuCl_2$, respectively [56]. According to Fig. 4.15, the copper rejection of $CuSO_4$ and $CuCl_2$ for the PBI NF membrane at a constant pressure of 10 bar and at pH 4.5 is 99.2% and 92.5%, respectively. These results indicate that PBI membranes exhibit better performance than the commercial NF membranes in terms of the rejections under similar operating conditions.

In summary, the PBI NF membranes fabricated in this work have comparable or even better performance than commercial membranes for the separation of phosphate, arsenate,

arsenite and copper ions. The PBI NF membrane is also a promising candidate for the separation of borate ions.

4.4 Summary

Polybenzimidazole nanofiltration membrane is clearly verified as an amphoteric charged membrane by the V-shape trend of NaCl rejection under different pH values due to the amphoteric imidazole groups within PBI molecules. Rejection performance of phosphate, arsenate, arsenite and borate ions shows the rejection of theses toxic anions is strongly dependent on the pH because solution pH determines the major species of these anions, their sizes, and the surface charge characteristics of the PBI membranes in aqueous solution. Divalent heavy metal cations, Cu(II), can be effectively removed by this PBI hollow-fiber membrane from their sulfate salt and chloride salt solutions, whose rejections are dependent on the solution pH and the accompany anions. Comparison with other commercial membranes indicates that the PBI NF membranes have comparable or better separation performance for P, As and Cu removal. The PBI NF membrane is a promising candidate for boron removal.

References

[1] S. Irdemez, N. Demircioglu, Y.S. Yidiz, Z. Bingul, The effects of current density and phosphate concentration on phosphate removal from wastewater by electrocoagulation using aluminum and iron plate electrodes, Sep. Purif. Techol. **52** (2006) 218-223.

[2] K. Kuzawa, Y.J. Jung, Y. Kiso, T. Yamada, M. Nagai, T.G. Lee, Phosphate removal and recovery with a synthetic hydrotalcite as an adsorbent, Chemosphere 62 (2006) 45-52.

[3] H. Carlsson, H. Aspegren, N. Lee, A. Hilmer, Calcium phosphate precipitation in biological phosphorus removal systems, Water Res. **31** (1997) 1047-1055.

[4] S. Tanada, M. Kabayama, N. Kawasaki, T. Sakiyama, T. Nakamura, M. Araki, T. Tamura, Removal of phosphate by aluminum oxide hydroxide, J. Colloid. Interf. Sci. **257** (2003) 135-140.

[5] A.E. Yilmaz, R. Boncukcuoglu, M.T. Yilmaz, M.M. Kocakerim, Adsorption of boron from boron-containing wastewaters by ion exchange in a continuous reactor, J. Hazard. Mater. **117** (2005) 221-226.

[6] R. Boncukcuoglu, A.E. Yilmaz, M.M. Kocakerim, M. Copur, An empirical model for kinetics of boron removal from boron-containing wastewaters by ion exchange in a batch reactor, Desalination **160** (2004) 159-166.

[7] A.E. Yilmaz, R. Boncukcuoglu, M.M. Kocakerim, B. Keskinler, The investigation of parameters affecting boron removal by electrocoagulation method, J. Hazard. Mater. **125** (2005) 160-165.

[8] N. Nadav, Boron removal from seawater reverse osmosis permeate utilizing selective ion exchange resin, Desalination **124** (1999) 131-135.

[9] T.S. Singh and K.K. Pant, Equilibrium, kinetics and thermodynamic studies for adsorption of As(III) on activated alumina, Sep. Purif. Technol. **36** (2004) 139–147.

[10] B. Tatineni and M. Hideyuki, Adsorption characteristics of As(III) and As(V) with titanium dioxide loaded Amberlite XAD-7 resin, Anal. Sci. **18**(2002) 1345–1349.

[11] E.O. Kartinen, C.J. Martin, An overview of arsenic removal processes, Desalination **103** (1995) 79-88.

[12] J. P. Chen, L. Yang, Study of a heavy metal biosorption onto raw and chemically modified Sargassum sp via spectroscopic and modeling analysis, Langmuir **22** (2006) 8906-8914.

[13] H. Genc-Fuhrman, P.S. Mikkelsen, A. Ledin, Simultaneous removal of As, Cd, Cr, Cu, Ni and Zn from stormwater: Experimental comparison of 11 different sorbents, Water Res. **41** (2007) 591-602.

[14] R.W. Peters, Chelant extraction of heavy metals from contaminated soils, J. Hazard. Mater. **66** (1999) 151-210.

[15] E. Pehlivan, T. Altun, Ion-exchange of Pb^{2+}, Cu^{2+}, Zn^{2+}, Cd^{2+}, and Ni^{2+} ions from aqueous solution by Lewatit CNP 80, J. Hazard. Mater. **140** (2007) 299-307.

[16] K.H. Chu, M.A. Hashim, Adsorption of copper (II) and EDTA-chelated copper (II) onto granular activated carbons, J. Chem. Technol. Biot. **75** (2000) 1054-1060.

[17] N.Y. Dho, S.R. Lee, Effect of temperature on single and competitive adsorptions of Cu(II) and Zn(II) onto natural clays, Environ. Monit. Assess. **83** (2003) 177-203.

[18] N. Unlu, M. Ersoz, Adsorption characteristics of heavy metal ions onto a low cost biopolymeric sorbent from aqueous solutions, J. Hazard. Mater. **136** (2006) 272-280.

[19] G. Abate, J.C. Masini, Influence of pH, ionic strength and humic acid on adsorption of Cd(II) and Pb(II) onto vermiculite, Colloid Surface A **262** (2005) 33-39.

[20] M. A. Keane, The removal of copper and nickel from aqueous solution using Y zeolite ion exchangers, Colloid Surface A **138** (1998) 11-20.

[21] W.M. Wang, V. Fthenakis, Kinetics study on separation of cadmium from tellurium in acidic solution media using ion-exchange resins, J. Hazard. Mater. **125** (2005) 80-88.

[22] J.S. Liu, H. Chen, X.Y. Chen, Z.L. Guo, Y.C. Hu, C.P. Liu and Y.Z. Sun, Extraction and separation of In(III), Ga(III) and Zn(II) from sulfate solution using extraction resin, Hydrometallurgy **82** (2006) 137-143.

[23] H, Abu Qdais, H. Moussa, Removal of heavy metals from wastewater by membrane processes: a comparative study, Desalination **164** (2004) 105-110.

[24] R.Y. Ning, Arsenic removal by reverse osmosis, Desalination **143** (2002) 237-241.

[25] Y. Magara, A. Tabata, M. Kohki, M. Kawasaki, M. Hirose, Development of boron reduction system for sea water desalination, Desalination **118** (1998) 25-33.

[26] M. Khayet, J.I. Mengual, T. Matsuura, Porous hydrophobic/hydrophilic composite membranes-Application in desalination using direct contact membrane distillation, J. Membr. Sci. **252** (2005) 101-113.

[27] Q. Yang , T.S. Chung, Y.C. Xiao, K.Y. Wang, The development of chemically modified P84Co-polyimide membranes as supported liquid membrane matrix for Cu(II) removal with prolonged stability, Chem. Eng. Sci. **62** (2007) 1721-1729.

[28] Q. Yang, J. Jiang, T.S. Chung, N.M. Kocherginsky, Experimental and computational studies of membrane extraction of Cu(II), AICHE J. **52** (2006) 3266-3277.

[29] J. Lv, Q. Yang, J. Jiang, T.S. Chung, Exploration of heavy metal ions transmembrane flux enhancement across a supported liquid membrane by appropriate carrier selection, Chem. Eng. Sci. 2007, in press.

[30] K.Y. Wang, T.S. Chung, Fabrication of polybenzimidazole (PBI) nanofiltration hollow fiber membranes for removal of chromate, J. Membr. Sci. **281** (2006) 307-315.

[31] K. K. Sirkar, Membrane separation technologies: Current developments, Chem. Eng. Commun. **157** (1997) 145-184.

[32] H. Saitua, M. Campderros, S. Cerutti, A.P. Padilla, Effect of operating conditions in removal of arsenic from water by nanofiltration membrane, Desalination **172** (2005) 173-180.

[33] M.C. Shih, An overview of arsenic removal by pressure-driven membrane processes, Desalination **172** (2005) 85-97.

[34] S.M.C. Ritchie, D. Bhattacharyy, Membrane-based hybrid processes for high water recovery and selective inorganic pollutant separation, J. Hazard. Mater. **92** (2002) 21-32.

[35] R. Simons. Trace element removal from ash dam waters by nanofiltration and diffusion dialysis. Desalination **89** (1993) 325-341.

[36] K.Y. Wang, T.S. Chung, Polybenzimidazole Nanofiltration Hollow Fiber for Cephalexin Separation, AIChE J. **52**(2006) 1363-1377.

[37] Y.H. Xu and D.Y. Zhao, Removal of Copper from Contaminated Soil by Use of Poly(amidoamine) Dendrimers, Environ. Sci. Technol. **39**(2005) 2369-2375.

[38] E.R. Nightingale, Phenomenological theory of ion sovation. Effective radii of hydrated ions, J. Phys.Chem. **63** (1959) 1381-1387.

[39] A.W. Mohammad, R. Othaman, N. Hilal, Potential use of nanofiltration membranes in treatment of industrial wastewater from Ni-P electroless plating, Desalination **168** (2004) 241-252.

[40] M.Y. Kiriukhin and K.D. Collins, Dynamic hydration numbers for biologically important ions, Biophys. Chem. **99** (2002) 155–168.

[41] E.M. Vrijenhoek, J.J. Waypa, Arsenic removal from drinking water by a "loose" nanofiltration membrane, Desalination **130** (2000) 265-277.

[42] J.S. Newman, Electrochemical systems, Prentice Hall, New Jersey, 2nd edn., 1991.

[43] K.Y. Wang, T. S. Chung, R. Rajagopalan, Novel Polybenzimidazole (PBI), Nanofiltration Membranes for the Separation of Sulfate and Chromate from High Alkalinity Brine To Facilitate the Chlor-Alkali Process, Ind. Eng. Chem. Res. **46** (2007) 1572-1577.

[44] S. Singh, K. Khulbe, T. Matsuura, P. Ramamurthy, Membrane characterization by solute transport and atomic force microscopy, J. Membr. Sci. **142**(1998) 111- 127.

[45] M. Mulder, Basic Principles of Membrane Technology, 2nd ed., Kluwer Academic Publishers, Dordrecht, 1996.

[46] O. Kedem and A. Katchalsky, Thermodynamic analysis of the permeability of biological membranes to non-electrolytes, Biochim. Biophys. Acta **27** (1958) 229-246.

[47] K. S. Spiegler, O. Kedem, Thermodynamics of hyperfiltration (reverse osmosis): criteria for efficient membranes, Desalination **1** (1966) 311-326.

[48] X.L. Wang, T. Tsuru, M. Togoh, S.I. Nakao, S. Kimura, Evaluation of pore structure and electrical properties of nanofiltration membranes, J. Chem. Eng. Jpn. **28** (1995) 186-192.

[49] K. Y. Wang, T.S. Chung, The characterization of flat composite nanofiltration membranes and their applications in the separation of Cephalexin, J. Membr. Sci. **247** (2005) 37–50.

[50] R. Weber, H. Chmiel, V. Mavrov, Characteristics and application of ceramic nanofiltration membranes, Ann NY Acad. Sci. **984** (2003) 178-193.

[51] R. Weber, H. Chmiel, V. Mavrov, Characteristics and application of new ceramic nanofiltration membranes, Desalination **157** (2003) 113-125.

[52] P.P. Power, W.G. Woods, The chemistry of boron and its speciation in plants, Plant Soil **193** (1997) 1-13.

[53] D. Prats, M. F. Chillion-Arias, M. Rodriges-Pastor, Analysis of the influence of pH and pressure on the elimination of boron in reverse osmosis, Desalination **128** (2000) 269-273.

[54] M.R. Pastor, A.F. Ruiz, M.F. Chillon and D.P. Rico, Influence of pH in the elimination of boron by means of reverse osmosis, Desalination **140** (2001) 145 -152.

[55] D.X. Wang, M. Su, Z.Y. Yu, X.L. Wang, M. Ando, T. Shintani, Separation performance of a nanofiltration membrane influenced by species and concentration of ions, Desalination **175** (2005) 219-225.

[56] K. Mehiguene, Y. Garba, S. Taha, N. Gondrexon, G. Dorange, Influence of operating conditions on the retention of copper and cadmium in aqueous solutions by

nanofiltration: experimental results and modeling, Sep. Purif. Technol. **15** (1999) 181-187.

[57] G. T. Ballet, L. Gzara, A Hafiane, M. Dhahbi, Transport coefficients and cadmium salt rejection in nanofiltration membrane, Desalination **167**(2004) 369-376.

[58] E.M. van Voorthuizen, A. Zwijnenburg, M. Wessling, Nutrient removal by NF and RO membranes in a decentralized sanitation system, Water Res. **39** (2005) 3657-3667.

[59] C. Visvanathan, P.K. Roy, Potential of nanofiltration for phosphate removal from wastewater, Environ. Technol. **18** (1997) 551-556.

[60] Y. Sato, M. Kang, T. Kamei, Y. Magara, Performance of nanofiltration for arsenic removal, Water Res. **36** (2002) 3371-3377.

[61] P. Dydo, M. Turek, J. Ciba, J. Trojanowska, J. Kluczka, Boron removal from landfill leachate by means of nanofiltration and reverse osmosis, Desalination **185** (2005) 131-137.

[62] Y. Ku, S.W. Chen, W.Y. Wang, Effect of solution composition on the removal of copper ions by nanofiltration, Sep. Purif. Technol. 43 (2005) 135-142.

5. CHAPTER FIVE

CONCLUSION AND RECOMMENDATIONS

5.1 Conclusion

The important findings, results and conclusions for different aspect of this work are derived and summarized as below.

5.1.1 Supported Liquid membrane Systems for Cadmium Removal

1. Quantum chemical computation can be proposed for carrier selection in supported liquid membrane (SLM) systems for heavy metal ions removal.

2. In the supported liquid membrane systems, heavy metal transmembrane flux can be enhanced effectively (with a flux increase by 91% in our case) by adding only small amount of anion(s) with less negative free energy of hydration.

3. The optimal conditions in our investigated SLM system for Cd(II) removal are as follows: membrane phase, 50 vol/vol % Aliquat 336 in an impregnated PTFE membrane; stripping phase, 1mM EDTA; stirring speed, 400rpm.

4. A separation factor of 15.7 for Cd(II) over Zn(II) is achieved and the stability of this SLM system is promising for future practical application.

5.1.2 Polybenzimidazole Nanofiltration Membrane for Water and Wastewater Treatment

Polybenzimidazole nanofiltration membrane is clearly verified as an amphoteric charged membrane by the V-shape trend of NaCl rejection under different pH values due to the amphoteric imidazole groups within PBI molecules. Rejection performance of phosphate, arsenate, arsenite and borate ions shows the rejection of theses toxic anions is strongly dependent on the pH because solution pH determines the major species of these anions, their sizes, and the surface charge characteristics of the PBI membranes in aqueous solution. Divalent heavy metal cations, Cu(II), can be effectively removed by this PBI hollow-fiber membrane from their sulfate salt and chloride salt solutions, whose rejections are dependent on the solution pH and the accompany anions. Comparison with other commercial membranes indicates that the PBI NF membranes have comparable or better separation performance for P, As and Cu removal. The PBI NF membrane is a promising candidate for boron removal.

5.2 Recommendations

The use of supported liquid membrane (SLM) for the removal of metal ions from wastewaters has been proposed as a promising separation technique [1, 2]. Supported liquid membrane (SLM) appears to be a promising method because it potentially offers a lot of advantages over other conventional separation technologies, such as easy operation,

low capital and operating costs, low energy consumption, continuous operation, high selectivity, relatively high fluxes, combination of extraction, stripping and regeneration processes into a single stage, uphill transport against concentration gradients, and small usage of amounts of extractants. SLM has received considerable attention over the past few decades and it has been demonstrated as an effective tool for the selective separation and recovery of resources from dilute solutions, particularly for the removal and recovery of metal ions. However, there have been very few large industrail applications of SLM due to lack of stability although SLMs have been widely studied for the separation and concentration of a variety of compounds. Various mechanisms have been proposed for SLM instability: loss of carrier from the oganic phase by dissolution, memabrane pores wetting, pressure difference or osmotic pressure gradient over the membrane [3, 4], and attrition of the organic film [5] or emulsion formation [5, 6]. SLM stability is also affected by the type of memrbane support and its pore size [7], organic solvent for the carrier, preparation method [8], etc.

PVDF (poly (vinylidene fluoride) (HSV 900), as proposed, could be used as the polymeric microporous support for SLM preparation with a reasonably high stability. Because of its superior chemical resistance and high hydrophobicity, it may have potential to possess the ability to separate two aqueous solutions in harsh chemical environments with prolonged stability. To prove this hypothesis, both symmetric and asymmetric membranes can be fabricated by both casting and solution spinning using the phase inversion method to study: 1) the science and engineering of solution spinning of flat PVDF microporous membranes; 2) the possibility of the enhancement of the stability of the spun PVDF membrane using in SLM systems; 3) Effect of various nonsolvent

additives, including Ethanol, Methanol, water, dodecane on membrane structure, stability and performance for cadmium removal; 4) Effect of the spinning conditions, including the temperature and the nonsolvent additive concentration on the membrane structure, stability and separation performance for cadmium removal.

References

[1] Ho WSW, Sirkar KK. Membrane Handbook, New York: Chapman & Hall, 1992.

[2] Juang RS, Chen JD, Huan HC. Dispersion-free membrane extraction: case studies of metal ion and organic acid extraction. Journal of Membrane Science. 2000;165(1): 59-73.

[3] Neplenbroek AM, Bargeman D, Smolders CA. Supported liquid membranes - Instability effects. Journal of Membrane Science. 1992; 67(2-3): 121-132.

[4] Kemperman AJB, Bargeman D, vandenBoomgaard T, Strathmann H. Stability of supported liquid membranes: State of the art. Separation Science and Technology. 1996; 31(20): 2733-2762.

[5] Neplenbroek AM, Bargeman D, Smolders CA. Mechanism of supported liquid membrane degradation - emulsion formation. Journal of Membrane Science. 1992; 67(2-3): 133-148.

[6] Dreher TM, Stevens GW. Instability mechanisms of supported liquid membranes. Separation Science and Technology. 1998; 33(6): 835-853.

[7] Chiarizia R. Stability of supported liquid membranes containing long-chain aliphatic-amines as carriers. Journal of Membrane Science. 1991; 55(1-2): 65-77.

[8] Yang XJ, Fane T. Effect of membrane preparation on the lifetime of supported liquid membranes. Journal of Membrane Science. 1997; 133(2): 269-273.

LIST OF PUBLICATIONS

1. J.W. LV, Q Yang, J Jiang, TS Chung, Exploration of heavy metal ions transmembrane flux enhancement across a supported liquid membrane by appropriate carrier selection. Chemical Engineering Science, **62** (2007) 6032 – 6039.

2. J.W. LV, KY Wang, TS Chung, Characterization and Investigation of Amphoteric PBI Nanofiltration Hollow Fibers for the Separation of P, B, As and Cu Ions. Journal of Membrane Science, **310** (2008) 557–566.

3. J.W. LV, Q Yang, J Jiang, TS Chung, Carrier Selection To Enhance Heavy Metal Ions Transmembrane Flux Through A Supported Liquid Membrane System, presented in AIChE Annual Meeting 2007, Salt Lake City, USA, 07-09 Nov 2007.